

KARMA



Karst Aquifer Resources availability and quality in the **Mediterranean Area**

Preliminary Water Budget

Deliverable 2.1

Authors:

Juan Antonio Barberá Fornell (UMA), Christelle Batiot-Guilhe (UMO), Rachida Bouhlila (ENIT), Michele Citton (AUB), Joanna Doummar (AUB), Emna Gargouri-Ellouz (ENIT), Hervé Jourde (UMO), Nesrine Laabidi (ENIT), Valeria Lorenzi (URO), José Francisco Martín Rodríguez (UMA), Bartolomé Andreo Navarro (UMA), Jaime Fernández Ortega (UMA), Jihad Othman (AUB), Marco Petitta (URO), Jean-Luc Seidel (UMO), Fairouz Slama (ENIT), Xiaoguang Wang (UMO)

Date: April 2020



This project has received funding from the European Union's PRIMA research and innovation programme



PRIMA
PARTNERSHIP FOR INNOVATION AND RESEARCH
IN THE MEDITERRANEAN AREA

Project Partners



(Coordinator)



SAPIENZA
UNIVERSITÀ DI ROMA



Executive Summary

WP2 is in charge to evaluate water availability at five test sites using different methods. The three main tasks focus on recharge, discharge (monitored at karst springs) and the estimation of floodwater storage potential where appropriate. All partners have an active role, for monitoring their own study area and/or for overarching method developments and activities. A final task will be dedicated to the evaluation of groundwater budgets and related uncertainties.

In this document we refer to Task 2.1 (Recharge assessment and tracer tests), whose activities include a preliminary assessment of the water budget (recharge/discharge) for each test site, using available data and information. This requires a critical analysis of information, to correctly identify potential gaps in knowledge. By this way, aquifers and springs having a different degree of knowledge can be selected for monitoring (Task 2.2).

The core activity of Task 2.1 will be the estimation of recharge of karst systems, by the adoption of an improved version of APLIS method, realized by UMA, which provides a distributed map at catchment scale of the recharge in the studied areas. The second method for validating the recharge evaluation is based on the use of water stable isotopes (URO, UMA, AUB, ENIT). By this way, the consistency of the recharge area with isotope values will be checked and the related conceptual model of groundwater flow will be refined. Additionally, in mature karst systems, the direct method based on tracer tests will be adopted, to verify input/output correlations.

The content of this document is a preliminary assessment of the water balance for each test site, based on literature or experimental data previously collected will be addressed. By this way, possible knowledge gaps will be identified and the list of the springs to be monitored will be defined.

The five selected study areas are the following

- To raise awareness on the project and its goals: letting the general public, policymakers and potential end-users know what we are doing during the project's lifetime, why it is important, and showing how PRIMA funding contributes to tackling societal challenges;
- To engage with potential end-users: getting familiar with their needs and ideas on the project, in an overall attempt to possibly adapt the main project outputs to their special requirements, acquire their support to operational WPs and their interest in future use of the project outputs;
- To disclose and promote our outputs and results: this will help to generate constructive feedback on the overall procedures and achievements of the project at an early stage, allowing conceivably needed adjustments, and later on facilitating the future utilization of its results.

In the following chapters the state-of-the-art on recharge assessment in each study area is shown, including references, to allow the correct implementation of the following activities inside WP2, also contributing to WP3 and WP4.

Table of Content

| | |
|--|----|
| Technical References | 1 |
| Version History | 1 |
| Project Partners | 1 |
| Executive Summary..... | 1 |
| Table of Content | 1 |
| 1. Introduction | 2 |
| 2. Gran Sasso Aquifer, Central Italy (Case Study Italy)..... | 3 |
| 2.1. Field site description..... | 3 |
| 2.2. Preliminary water budget | 8 |
| 2.3. Discussion and Conclusion | 13 |
| 2.4. References | 16 |
| 3. The Qachqouch aquifer (Case study Lebanon) | 18 |
| 3.1 Field site description – river and spring..... | 18 |
| 3.2 Catchment monitoring, data collection and analysis | 20 |
| 3.3 Preliminary water budget and catchment delineation..... | 21 |
| 3.4 Current activities related to Water Balance Assessment | 23 |
| 3.5 References | 23 |
| 4. The Eastern Ronda Mountains (study area in Spain) | 24 |
| 4.1 Field site description..... | 24 |
| 3.2 Preliminary water budget | 28 |
| 4.3 Discussion and Conclusion | 34 |
| 4.4 References | 35 |
| 5. Lez Karst Catchment, France | 37 |
| 5.1 Field site description..... | 37 |
| 5.2 Available Dataset..... | 39 |
| 5.3 Preliminary water budget | 39 |
| 5.4 References | 42 |
| 6. Djebel Zaghouan aquifer, Tunisia | 44 |
| 6.1 Field site description..... | 44 |
| 6.2 Water resources | 46 |
| 6.3 Preliminary water budget | 47 |
| 6.4 Conclusion..... | 50 |
| 6.5 References | 50 |

1. Introduction

The overarching objective of the KARMA project is to achieve substantial progress in the hydrogeological understanding and sustainable management of karst groundwater resources in the Mediterranean area in terms of water availability and quality.

At the scale of the entire region, the main objective is to accomplish the first consistent and detailed **Mediterranean Karst Aquifer Map and database** (MEDKAM). MEDKAM will include detailed information related to aquifer type, recharge, vulnerability to contamination and groundwater-dependent ecosystems (GDE), and will allow to perform more advanced analyses with respect to floodwater storage and water stress under conditions of global change (climate change, land-use change, population increase).

At the catchment or aquifer scale, the objective is to advance and compare transferable **modeling tools** for improved predictions of climate-change impacts and better-informed water management decisions, and to prepare **vulnerability maps** as tools for groundwater quality protection. Hydrological monitoring, isotope studies and tracer tests will be carried out to achieve better hydrogeological understanding and to obtain data for the calibration and validation of models and vulnerability maps.

At the scale of individual springs, the objective is to develop and implement **monitoring and early-warning systems** (EWS) for groundwater contamination, focusing on short-term contamination events, but also addressing long-term trends.

The project is structured into five work packages (WPs), led by different project partners, according to their key expertise. **WP1** deals with project management, communication and dissemination. **WP2** focuses on water availability and includes recharge assessment, spring discharge monitoring, assessment of floodwater storage potential and an evaluation of water budgets and the related uncertainties. **WP3** focuses on water quality, including the installation of a water-quality monitoring network (related to discharge monitoring in WP2), early-warning systems for spring-water contamination, vulnerability mapping and an assessment of groundwater-dependent ecosystems. **WP4** deals with the advancement of modeling tools, including artificial neural networks, lumped-parameter models and distributed models. **WP5** focuses on the development of the Mediterranean Karst Aquifer Map and database (MEDKAM).

The main objective of WP2 is the assessment of groundwater availability by investigating recharge, discharge and storage at five karst aquifer systems (test sites) in different countries. Evaluation will be on yearly basis, seasonal scale and event scale, considering previously available data and extensive monitoring data collected during the project. To reach these goals, water availability at our five test sites will be evaluated using different methods. The three main tasks focus on recharge, discharge (monitored at karst springs) and the estimation of floodwater storage potential where appropriate. All partners have an active role, for monitoring their own study area and/or for overarching method developments and activities.

This document (D2.1) refers to Task 2.1 (Recharge assessment and tracer tests) and includes a preliminary assessment of the water budget (recharge/discharge) for each test site, based on literature or experimental data previously collected will be addressed. By this way, possible knowledge gaps will be identified and the list of the springs to be monitored will be defined. All partners have provided the state-of-the-art on recharge assessment in each study area, as described in the following chapters. Starting from this common knowledge base, the further activities previewed in Task 2.1 and in the entire WP2 will be correctly developed, offering also relevant insights for WP3 and WP4.

2. Gran Sasso Aquifer, Central Italy (Case Study Italy)

2.1. Field site description

The study area selected for the KARMA project in Italy is the Gran Sasso carbonate fractured and karstified aquifer, located in Central Italy, inside the National Park of “Gran Sasso and Maga Mountains”.

Gran Sasso hydrostructure is defined as a single basal regional aquifer of about 700 km² of total extension of carbonate outcrops, within a total area of the ridge wider than 1000 km². It can be considered as a calcareous-karstic aquifer system and it is one of the most representative karst aquifers of the Apennines, in detail of the central-southern area of Italy. This relevance is due to the conspicuous amount of water resources deeply exploited for any purpose, the interaction of infrastructures with the surface and the groundwater and, finally, to the enhancement and protection of protected areas (Monjoie, 1980).

The interest of this area is linked not only to the great availability of groundwater resources but also to both anthropogenic problems, such as the construction of the Gran Sasso motorway tunnel and in the morphology characteristics of the karst system. The specific problems and pressures associated with the area of interest were also taken into consideration, such as seismicity of the area and the construction of the Gran Sasso motorway tunnel, which led to important changes in the area's groundwater circulation. The strategic role of the karst system is defined by the high quality of the water, guaranteed also by a limited anthropization of the territories in which they generally develop, and by the water quantities that these systems are able to contain.

The Gran Sasso aquifer is characterized by meso-Cenozoic carbonatic units of a Lazio-Abruzzi platform, associated with silico-calcareous-marly lithologies, of the same age, referable to basin environments and transition to the Umbrian-Marchean basin (Accordi et al., 1988). The stratigraphy and the structural elements (i.e. the presence of dolomitic deposits, the marly lithotypes with lower permeability and the high number of main faults) affect the characteristics of the Gran Sasso calcareous complex, permeable for fracturing and karstification. These elements often act as an obstacle to the groundwater flow causing the presence of different groundwater watersheds and influencing the direction of the flow paths. In correspondence to the high structures, the fractured dolomites have a hydraulic conductivity lower than that of the limestones (10⁻⁸-10⁻⁹ ms⁻¹) and may constitute an obstacle to the discharge of groundwater (Monjoie, 1980). Permeability limits are constituted to the main overthrust, located in the northern and eastern areas, with direction E-W and then N-S, dipping respectively to the South and West. The overthrust has therefore caused a tectonic lifting of the carbonate Units of the platform Meso-Cenozoic, which represent the regional aquitard, on terrigenous turbidites ones of Mio-Pliocene, which represent the regional aquiclude (no flow limit) (Figure 1). The limits of the hydrogeological structure of the Gran Sasso aquifer are well defined on both the northern and eastern sides. However, it is still not well defined the limit in the southwestern area and in detail the relationships with the hydrostructures of Mt Sirente and Mt Morrone, giving rise to groundwater exchanges (Petitta & Tallini, 2002).

The Gran Sasso aquifer feeds spring groups, located at different altitudes along the low permeability boundary, with a huge discharge of more than 18 m³/s (Adinolfi Falcone et al., 2008). These springs have been organized into six groups based on groundwater flow and hydrochemical characteristics, as illustrated in Figure 2.1 (Barbieri et al., 2005). The springs of group A are fed on the northern boundary, lying near the no-flow limit due to the main thrust, while the springs of group B have an unsteady and low discharge because they are fed by local perched aquifers. The main springs of the Gran Sasso massif lie at its southern border (elevation below 650 m asl), at the southwestern boundary of the

Preliminary Water Budget

L'Aquila plain (group D; Petitta, 2003) and along the Tirino River valley (south-eastern boundary, group E), whose springs are in the remote discharge area. Springs of group C show evidence of fast groundwater flow, directly connected with the aquifer core. The spring groups A and C lie close to and in axis with the motorway tunnels and their discharge declined after tunnel boring and consequent groundwater drainage. Finally, the groundwater sampled from the tunnels and the related underground laboratories (group F) is characterized by low electrical conductivity (Petitta, 2002). Discharge from the Gran Sasso springs has decreased significantly after tunnel excavation in the 1980s and subsequent groundwater drainage and probably also as a result of climate change (Dragoni, 1998; Massoli Novelli, 1997). In subsequent years (1996–2000), spring discharge has risen slightly, indicating that the aquifer groundwater, also thanks to drainage by the tunnels, has reached a new steady-state (Petitta, 2002). A detailed evaluation of the single spring discharge is resumed in Table 2.1, and it has been published in the Hydrogeological Map of Gran Sasso Aquifer (Table 2.2).

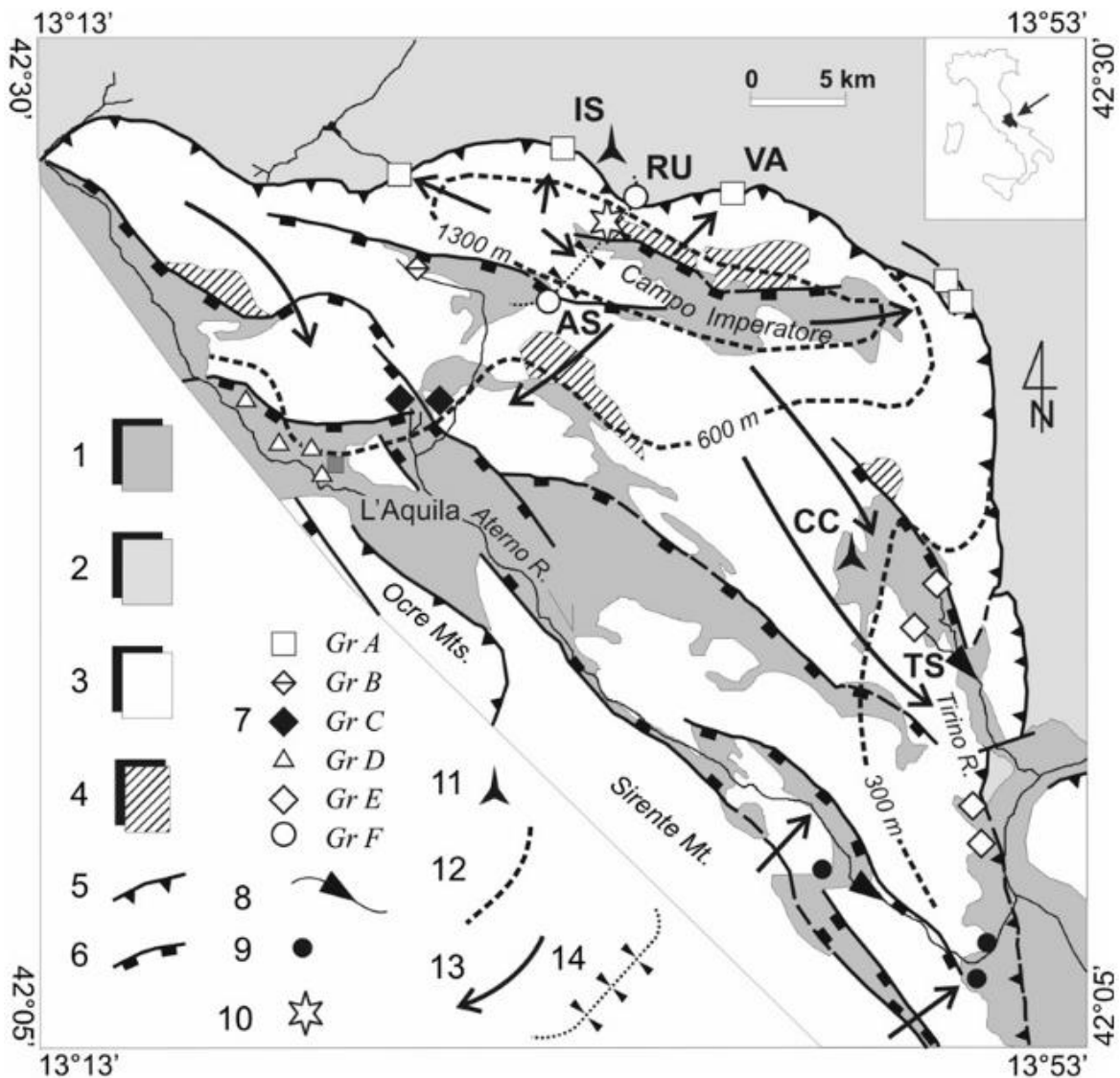


Figure 2.1 Gran Sasso hydrogeological outline. 1: aquitard (continental detrital units of intramontane basins, Quaternary); 2: aquiclude (terrigenous turbidites, Mio-Pliocene); 3: aquifer (calcareous sequences of platform Meso-Cenozoic); 4: low permeability substratum (dolomite, upper Triassic); 5: thrust; 6: extensional fault; 7: main spring; AS: Assergi drainage; RU: Ruzzo drainage; VA: Vacelliera spring; TS: Tirino springs; symbols refer to the six spring groups identified in Barbieri et al. (2005); 8: linear spring; 9: springs belonging to a nearby aquifer; 10: INFN underground laboratories (UL in the text); 11: meteorological station (IS: Isola Gran Sasso, CC: Carapelle Calvisio); 12: presumed water table in m asl; 13: main groundwater flow path; 14: highway tunnels drainage. [Amoruso, 2012]

Preliminary Water Budget

Table 2.1 Discharge of the six groups of the springs in Gran Sasso aquifer. The discharge values refer to the 1970-1990 period (groups A and B) and to 1994-2000 one (groups C, D, E, and F) [Petitta, 2002].

| GROUP | DISCHARGE (m ³ /s) |
|-------|-------------------------------|
| A | 1.577 |
| B | 0.10 |
| C | 0.99 |
| D | 0.753 |
| E | 10.69 |
| F | 1.5 |

Table 2.2A detailed evaluation of the single spring discharge published in the Hydrogeological Map of Gran Sasso Aquifer. For groups 1 and 2 the measures relate to the period 1970-1990. for groups 3,4,5,6 the measures relate to the period 1994-2000 [Petitta, 2002].

| Class. | Sorgente | Quota (m) | Temperatura (°C) | Conducibilità El. (µs/cm) | Portata (L/s) |
|----------|--|-------------|------------------|---------------------------|---------------|
| Gruppo 1 | S1 Chiarino | 1315 | 5,7 | 306 | 80 |
| | S2 Rio Arno | 1524 | 3,9 | 310 | 100 |
| | S3 S. Nicola I | 1600 | 7,6 | 271 | 116 |
| | S4 S. Vittore I | 1600 | 7,0 | 305 | 156 |
| | S5 S. Vittore II | 1500 | 6,1 | 198 | 52 |
| | S6 Acqua Zeta | 1400 | 6,7 | 278 | 6 |
| | S7 Lama Bianca | 1300 | 5,4 | 198 | 55 |
| | S8 Fiumette | 1530 | 5,4 | 214 | 52 |
| | S9 Ruzzo | 750-1600 | 5,5 | 298 | 300 |
| | S10 Mortaio D'Angri | 650 | 7,4 | 263 | 280 |
| | S11 Vitella D'Oro | 690 | 7,5 | 216 | 380 |
| Gruppo 2 | S12 Acqua Santa | 730 | 10,1 | 418 | 42 |
| | S13 Fonte Della Forma | 1000 | 10,9 | 300 | 4 |
| | S14 Vagnatore | 900 | 9,3 | 333 | 7 |
| | S15 Spugna li | 940 | 9,6 | 363 | 5,4 |
| | S16 S. Pietro | 1150 | 9,5 | 295 | 0,1 |
| | S17 Costa Lata | 1010 | 7,2 | 199 | 5,2 |
| | S18 Santa Maria | 900 | 7,9 | 254 | 41 |
| | S19 Acquagrossa | 1200 | 11,0 | 208 | 3,5 |
| | S20 Fonte Annorsi | 1157 | 10,0 | 238 | 1,6 |
| | Gr. 3 | S21 Tempera | 650 | 7,8 | 237 |
| S22 Vera | | 650 | 7,9 | 238 | 190 |
| Gruppo 4 | S23 Scentella-Colle | 694 | 10,9 | 561 | 2 |
| | S24 Fontanile S. Giorgio | 669 | 14,7 | 587 | 5 |
| | S25 F.Te Vecchia-S. Vittorino | 675 | 13,3 | 512 | 0,1 |
| | S26 Collettara | 710 | 12,0 | 602 | 0,5 |
| | S27 Fonte Arconi - Cese | 685 | 10,4 | 621 | 0,2 |
| | S28 S. Giusta-Sassa | 677 | 12,6 | 772 | 0,1 |
| | S29 Casa Mannetti | 670 | 10,8 | 688 | 0,1 |
| | S30 Vetoio | 640 | 10,7 | 459 | 430 |
| | S31 Boschetto Italtel | 625 | 14,1 | 412 | 220 |
| | S32 Casa Buccella | 630 | 11,2 | 443 | 20 |
| | S33 Sidis-Staz. L'Aquila | 634 | 12,4 | 472 | 25 |
| Gruppo 5 | S34 99 Cannelle | 635 | 11,6 | 580 | 50 |
| | S35 Capo D'Acqua | 340 | 10,6 | 499 | 2800 |
| | S36 Presciano | 336 | 11,1 | 570 | 1900 |
| | S37 Franceschelli | 327 | 11,4 | 392 | 20 |
| | S38 Gruppo Del Viale | 325 | 11,3 | 385 | 25 |
| | S39 Scastello | 315 | 11,4 | 388 | 50 |
| | S40 Fontanelle | 310 | 11,2 | 380 | 400 |
| | S41 Basso Tirino | 300 | 12,0 | 544 | 5500 |
| | S42 S. Calisto | 300 | 11,6 | 560 | 2000 |
| | S43 S. Liberata | 255 | 11,5 | 530 | 500 |
| Gr. 6 | S44 Capo Pescara | 270 | 12,0 | 513 | 7000 |
| | S45 Lato L'Aquila (Progr. 0-5000m) | 967 | 6,1 | 223 | 450 |
| | S46 Lato Teramo (Progr. 5500-7000m) | 964 | 5,0 | 227 | 900 |
| | S47 Lato Teramo (Galleria Dei Servizi) | 960 | 5,0 | 233 | 150 |

The hydrogeological system can be divided into several hydrogeological complexes each characterized by a specific lithology and porosity, placed in contact with each other for stratigraphic and tectonic reasons (Figure 2.2). So, it is possible to recognize and evaluate hydrogeological differences between the various formations on the basis of lithological, sedimentological and structural characteristics and can be grouped into seven hydrogeological complexes with homogeneous characteristics. The hydrogeological complexes of the area take into consideration are: a) recent and ancient continental detrital deposits; b) continental debris Units; c) ancient continental debris Units; d) marine terrigenous Units; e) Marly complex, f) Limestone complex; g) Dolomite complex.

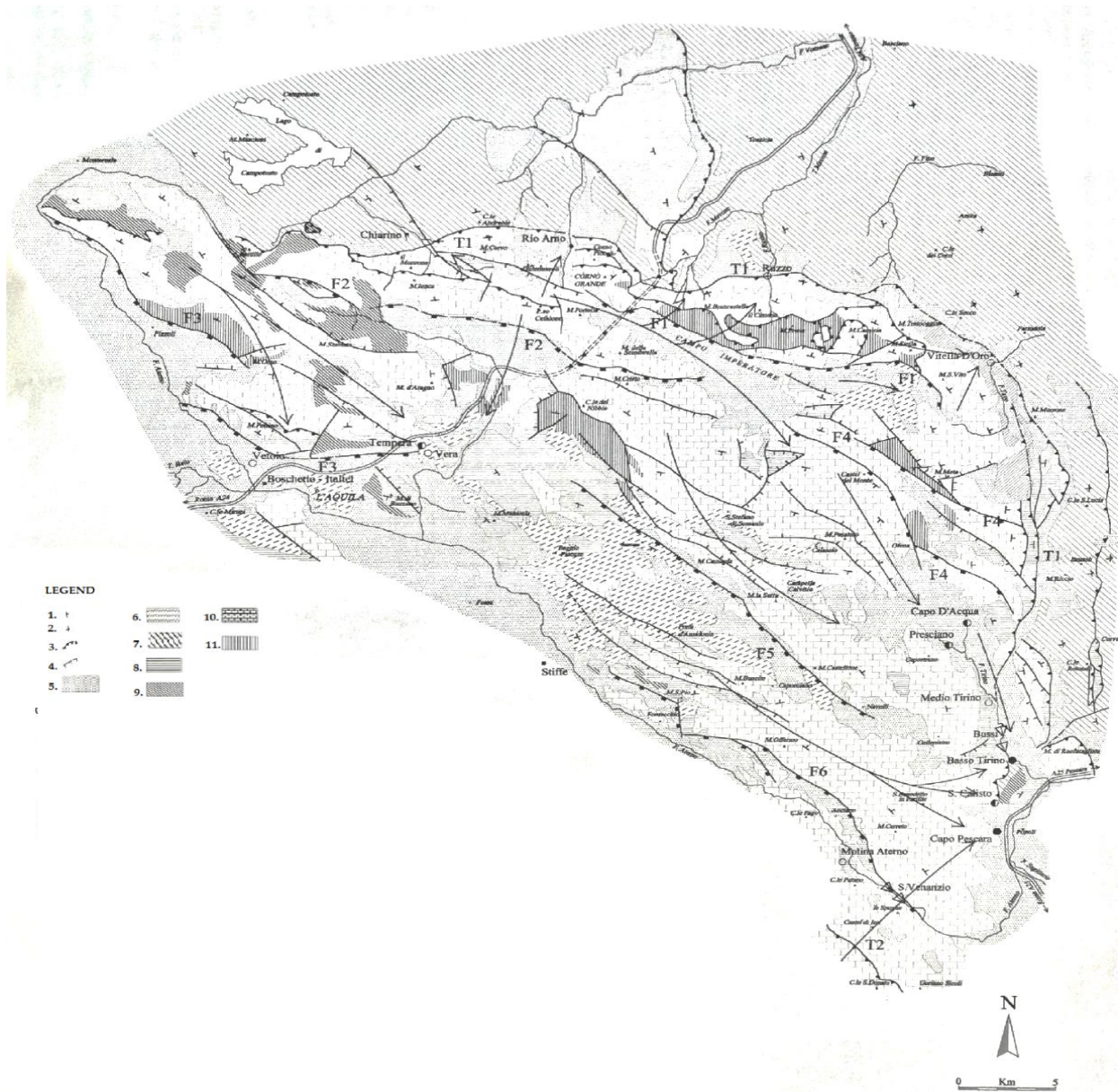


Figure 2.2 Hydrogeological scheme of The Gran Sasso massif. 1. Layering of the strata; 2. Inverted layers; 3. Thrust; 4. Normal fault; 5. The complex of recent and ancient continental detrital deposits; 6. The complex of recent continental debris Units; 7. The complex of the ancient continental debris Units, 8. The complex of marine terrigenous Units; 9. Marly complex, 10. Limestone complex; 11. Dolomite complex T1. zero flow permeability limit; T2. Tectonic limit of the Sirente hydrostructure; F1. Campo Imperatore fault; F2. Monte S. Franco-Valle Fredda fault; F3. Pizzoli-L'Aquila fault; F4. Castel del Monte-Capo d'Acqua fault; F5. Barisciano-Navelli Fault, F6. Valle dell'Aterno-Molina [modified from Tallini, M.; Petitta M.; Ranalli, D.,2000].

Preliminary Water Budget

Due to karst ducts promoting infiltration, groundwater moves vertically, in the unsaturated zone which has a vertical thickness of about 1000 m, ranging from 300 m to 1500 m, as shown in Figure 2.3. This movement within the aquifer is due to the presence of karst ducts that promote infiltration. Moreover, the speed and the quantity of the water inside the karst pipes depend on their width and on the outcrop lithology as shown in Figure 2.4. Then, it flows horizontally in the saturated zone to reach the main springs located at the aquifer boundary. The flow is predominantly a SE-trending (Petitta, 2002). The underground hydrodynamics of the carbonate massif is conditioned by the presence of important structural discontinuities and tectonic movements. This creates a series of intercommunicating basins that develop mainly along the NW-SE direction (Celico, 1983). The tectonic and structural discontinuities act as limits of permeability that cause variations in the water level of the regional aquifer. The Gran Sasso water table can, therefore, be defined as characterized by structural discontinuities or lithological variations that affect the flow of water but do not completely hinder it. Moreover, also the preferential directions of the groundwater flow are conditioned locally by the main tectonic discontinuities.

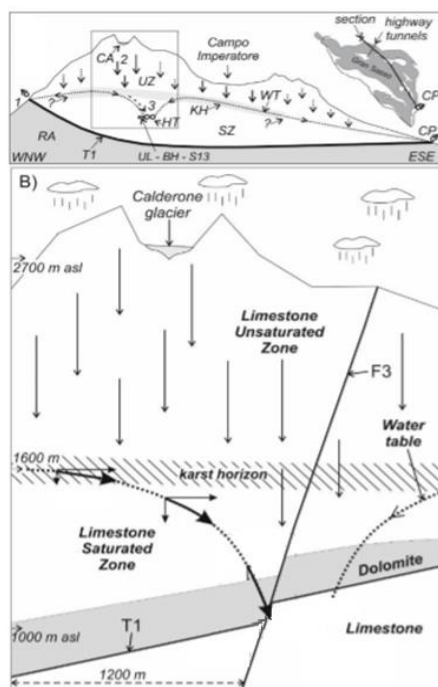


Figure 2.3 Scheme not on the scale of the Gran Sasso aquifer. UZ – unsaturated zone; SZ – saturated zone; KH – karst horizon; RA – regional aquiclude; T1 – permeability boundary (main lower thrust); WT – water table; CA – Calderone glacier; 1 – overflow spring (CP: Capopescara spring); 2 – preferential groundwater flow path area; 3 – preferential groundwaterflowing toward the UL; PR – preferential recharge; DR – diffuse recharge. [De Luca, Di Carlo, & Tallini, 2016]

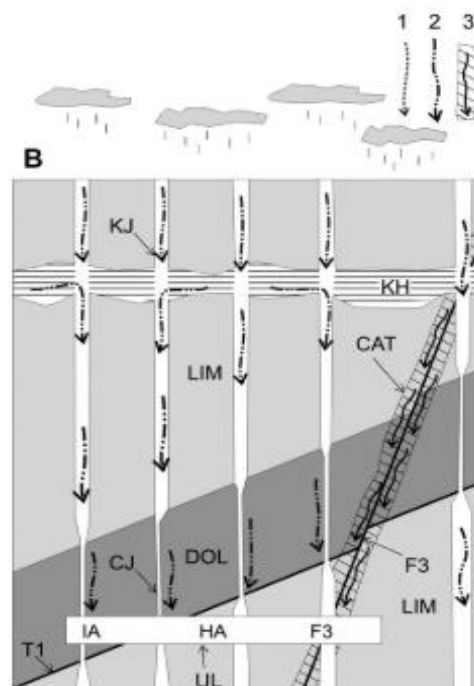


Figure 2.4 Cartoons not in scale representing groundwater infiltration. LIM – limestone; DOL – dolomite; T1 – thrust; F3 – main normal fault; CJ – close joint; KJ – open joint; KH – karst horizon; CAT – cataclastic associated to F3; IA – interferometer area; HA – hall A; fracture network flow (slow flow): 1 – base flow; 2 – recharge flow; 3: fast flow through discontinuities (F3) and associated cataclastic [Raffaele Adinolfi Falcone, Antonella Falgiani, 2006].

To sum up, the fracture conduit systems of the Gran Sasso aquifer are uniform and well interconnected, but only locally karstified to reach a conduit flow condition. As a result, the hydraulic conductivity tensors and the corresponding equivalent values were calculated for the surface rock mass. Results show equivalent hydraulic conductivity ranging from 3×10^{-3} m/s to 6×10^{-3} m/s, with a maximum value of 10–2 m/s and minimum value of 10–4 m/s. In accordance with borehole permeability tests, the hydraulic conductivity generally decreases with increasing depth (Scozzafava, 2001).

Preliminary Water Budget

Consequently, at the scale of the entire ridge, the Gran Sasso Aquifer can be considered as a hydrogeological basin subdivided in several sub-basins by the role of tectonic discontinuities, where the faults act frequently as groundwater divide: each sub-basins is feeding one main spring (as on the northern side) or a group of them (as on the southern side). The results of a tracer test performed during the excavation of the highway tunnel, confirms this conceptual model. From the end of 1971 to December 1972, in the Fontari deep borehole (located along the highway tunnel trace), a certain quantity of fluorescein, was introduced at the level of the water table, and then reported by fluorocaptors distributed in all the springs take into consideration. It was observed that after only 5 days the dye appeared on the Teramo side, ending after about a month and a half, while on the L'Aquila side the tracer was observed after 7-8 days and reprocessed for about a year. Moreover, the flow in the Apennine direction of a large part of the water mass was demonstrated by the appearance of the tracer at Capodacqua spring of about 30 km away, only 20 days after release, while at Rio Arno springs it was always negative because of the impermeable strata along the transversal faults.

The use of artificial tracers placed in the Fontari borehole allowed to verify a direct connection between the karst aquifer crossed by the tunnels and the main springs fed by the massif and then to outline the general characteristics of the geometry and underground hydrodynamics of the Gran Sasso hydrostructure, already described above (INFN-LNGS, 2018, INFN, 2018). The diffusion of the tracer even beyond the very fast arrival on the springs of the northern side confirms that the groundwater flow in the fractured system, tends to spread more widely involving different hydrogeological basins and related springs.

2.2. Preliminary water budget

As mentioned before, the karst-partitioned aquifer of Gran Sasso is about 700 km² wide. In the Gran Sasso aquifer two altitude belts were defined: the middle belt (MB) and the high one (HB) with elevations ranging from 1400 m to 1800 m and from 1800 m to 2900 m, respectively (Figure 2.5) (Amoruso, 2012).

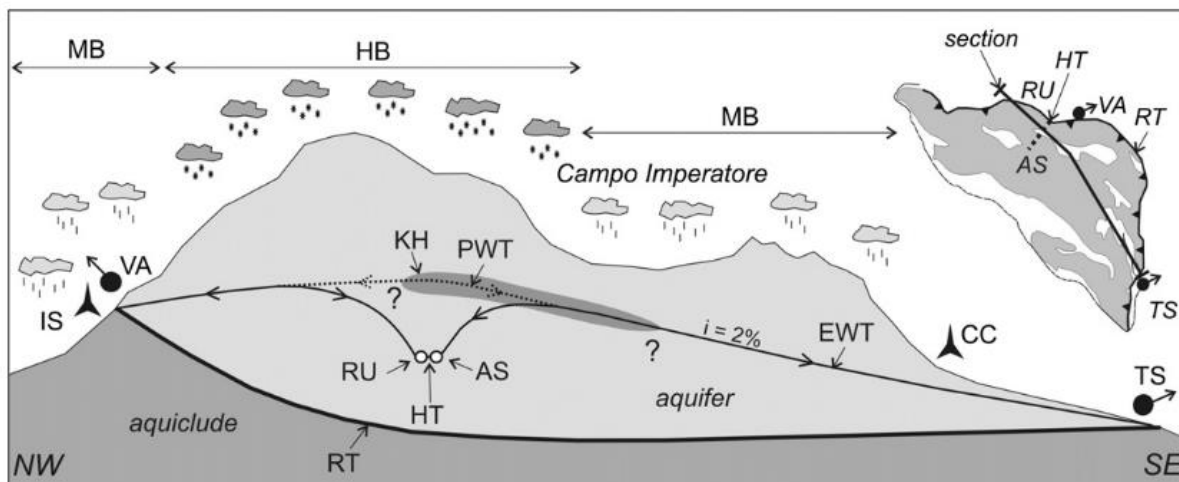


Figure 2.5 Gran Sasso aquifer hydrogeological scheme; VA: Vacelliera spring (projection); TS: Tirino springs; RU: Ruzzo drainage (projection); AS: Assergi drainage (projection); HT: highway tunnels; RT: regional thrust (permeability boundary); EWT: existing water table; PWT: previous water table (before tunnels boring); KH: karst horizon; HB: high belt; MB: middle belt [Amoruso,2012].

The location of the saturated zone corresponds to the karst horizon (KH), as shown in Figure 2.5, established during the project of the motorway tunnel (1200–1300 m asl) (Anas-Cogefar, 1980), as confirmed by measurements of head pressure in the UL (Underground Laboratory for Nuclear Physics), about 25–30 atm at the tunnel altitude of 970 m asl. Moreover, the karst horizon is characterized by

the presence of the water table depth and by the presence of main faults (Adinolfi Falcone et al., 2008). From a hydrogeological point of view, the UL represents a "window" on the saturated zone in the core of the aquifer, under the zone of oscillation of the water table (which varies from 300 to 1500 m). At this time, numerous hydrogeological data have been collected, relating to the construction phases of underground structures (1960-1970) and the following monitoring activities (Petitta et alii, 2002; Barbieri et alii, 2005; Adinolfi Falcone et alii, 2008; Tallini et alii, 2013). Consequently, considering that the Gran Sasso aquifer is karstified in its saturated zone and has very limited evolved karst conduit systems, it may be assumed that on the regional scale, the groundwater flow is gravity-driven (White 2003), (Tallini et alii, 2013), (Toth 1963).

The Gran Sasso aquifer has been studied in detail over the last 15 years (Galassi et al., 2014; Tallini et al., 2014), revealing a unique regional, locally partitioned structure, characterized by gravity-driven groundwater flow (Tallini et al., 2013). Most of the Gran Sasso aquifer mean discharge (23 m³/s: Amoruso et al., 2013) occurs at the southeastern sector of the massif, where the springs of the Pescara River are located (Figure 2.6). In previous studies, Massoli Novelli et al. (1999) inferred that the Gran Sasso aquifer discharge at the River Pescara spring system occurs predominantly at the Capo Pescara spring. The Capo Pescara is supposed to be fed predominantly by the Sirente aquifer (Massoli Novelli et al., 1999), which is hydraulically in contact with the Gran Sasso ridge, where the spring system of the River Pescara is located. The southernmost sector of the Sirente aquifer has hydrogeological features in terms of recharge similar to the Gran Sasso aquifer, with a mean discharge of 8 m³/s. Consequently, as already hypothesized by Massoli Novelli et al. (1999), the Capo Pescara spring unit recharge may be attributed to groundwater originating predominantly from the Sirente aquifer, without excluding a possible minor contribution from the Gran Sasso aquifer. Moreover, the larger Capo Pescara discharge should come to Sirente aquifer, through groundwater seepage towards the Gran Sasso aquifer, based on assessments of the hydrological balance (Scozzafava, 2001). The possibility of unique identification of the catchment area of each spring result particularly difficult due to lack of hydrogeological discontinuity in the Gran Sasso SE sector (Massoli Novelli, 1999).

The evaluation of the Gran Sasso water budget is based on the dominant element represented by the value of effective infiltration, as "that fraction of meteoric water that penetrates the subsoil so deeply that it feeds an aquifer of regional interest" (Boni et al., 1986) and which expresses the capacity of a hydrogeological complex to absorb meteoric water, subtracting it from the runoff. This value does not depend only on lithology, but to a large extent also on local climatic conditions. In fact, in the hydrogeological setting of Gran Sasso, infiltration processes are those of typical karst areas, with a high recharge rate, directly influenced not only by rainfall but also by seasonal snow soil coverage. These characteristics reflect in the water budget calculations, proposed by the Authors following different methods.

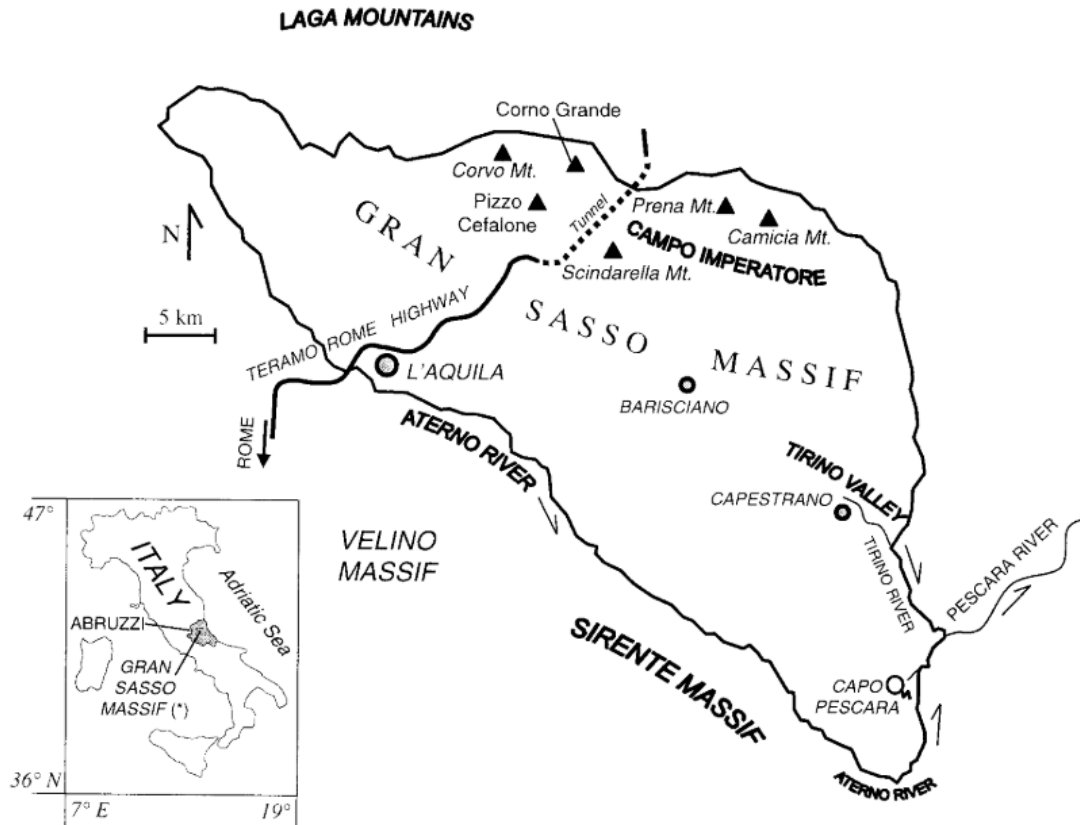


Figure 2.6 Location of the Pescara River and Capo Pescara spring [Massoli Novelli, 1999].

In fact, there are several ways to calculate the water budget. For example, the method of "direct" assessment of effective infiltration. This type of method is based on the concept that the amount of water that on average emerges from the subsoil is equivalent to the amount that on average penetrates it on an annual basis. The flow rate of the springs can be traced back to the value of effective infiltration expressed in millimeters/year. To estimate the water budget at the scale of the entire the Gran Sasso aquifer, this method has been used (Boni et al., 1986).

Thus, an alternative way to study the Gran Sasso water budget with higher detail and larger scale is to apply indirect methods. The methodology applied by Scozzafava & Tallini (2001) to determine the effective infiltration of the Gran Sasso aquifer, provides for the application of the Thornthwaite method (Thornthwaite & Mather, 1957) modified according to local hydrogeological characteristics. More specifically, to investigate the distribution of net infiltration and to identify directions of groundwater flow, it has been used a procedure that includes several methods, principally the Thornthwaite (Thornthwaite and Mather, 1957) and curve-number (CN) methods (USDA–SCS 1986), which are partly modified (Scozzafava, 2001) (Figure 2.7). The Thornthwaite method has been modified to discriminate between runoff and net infiltration. The change involves the use of the CN parameter (USDA–SCS 1986; Boughton 1989), developed by the US Soil Conservation Service (SCS), for the evaluation of runoff. The process that was adopted is different from the one commonly used to compute recharge from net rainfall and hydrogeological soil data. With regard to net-infiltration evaluation, the CN method was successfully applied in water budgets of regional areas (mapped at greater than 1:50,000 scale) (Scozzafava, 2001). The modified (Thornthwaite + CN) method is simple and flexible to use and makes possible the determination of recharge in a complex hydrogeological system, such as the Gran Sasso karstic massif. Other components of the evaluation include the analysis

Preliminary Water Budget

of the location, timing and amount of snowmelt, and determination of the distribution of endorheic areas has been considered. The final product is the spatial distribution of net infiltration.

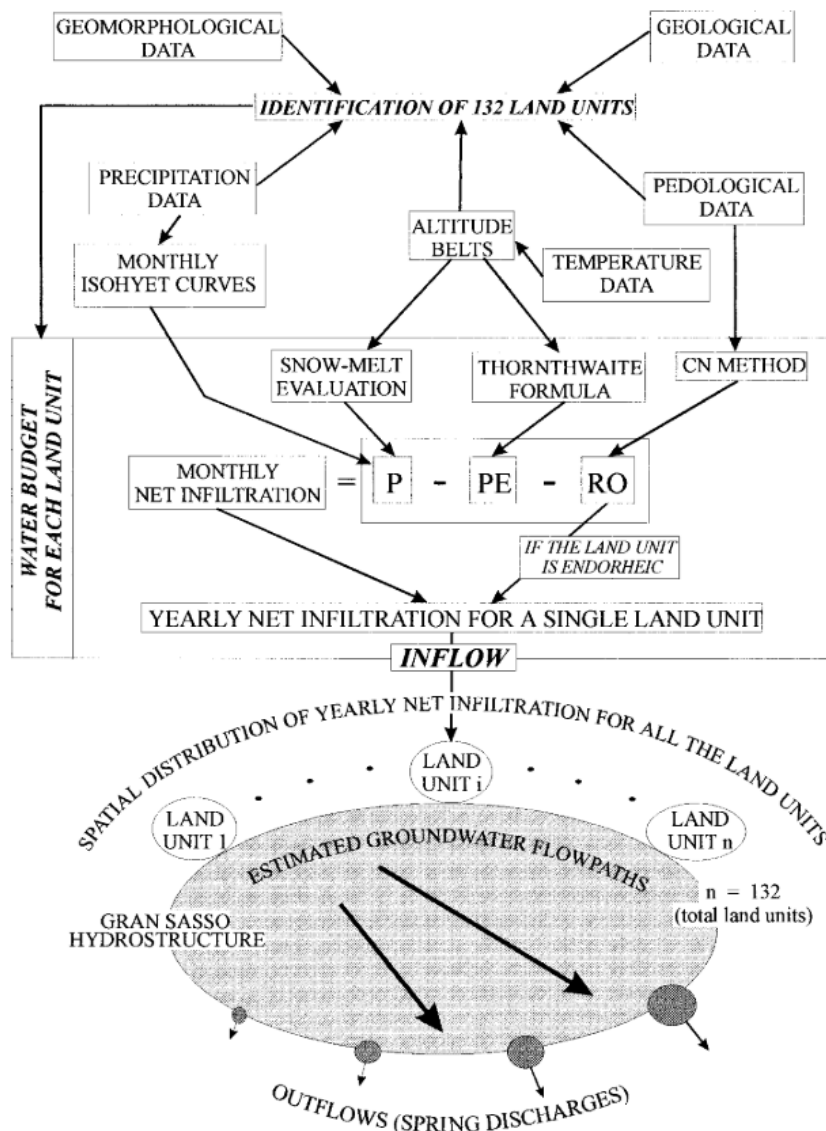


Figure 2.7 Flowchart of procedure and methods used for the evaluation of the spatial distribution of net infiltration in the Gran Sasso hydrogeological system [Scozzafava & Tallini, 2001].

The complete procedure to obtain the Gran Sasso water budget is made up of the following steps:

1. Analysis of precipitation data, including evaluation of average monthly rainfall;
2. Analysis of temperature data, including evaluation of average monthly temperature from the Thermo-pluviometric stations;
3. Evaluation of snow distribution in winter and snow-melt in spring; these data were used in the Thornthwaite water budget for each land unit;
4. Evaluation of potential evapotranspiration using the Thornthwaite formula for each land unit;
5. Analysis of pedological data including evaluation of the thickness, structure, texture, and hydromorphic characteristics of the main Gran Sasso soils;

Preliminary Water Budget

6. Evaluation of runoff using the CN method;
7. Calculation of the monthly Thornthwaite water budget for each land unit;
8. Calculation of yearly Thornthwaite water budget for each land unit and evaluation of the yearly spatial distribution of net infiltration;
9. Comparison between the spatial distribution of yearly net infiltration (inflows) and spatial distribution of the main spring discharges (outflows);
10. Inference of the groundwater flow paths.

In order to identify flowpaths, it was necessary to evaluate the spatial distribution of net infiltration. Moreover, the total amount of net infiltration approximately corresponds to the total recharge of groundwater, which greatly simplifies the computation of the water budget.

Regarding the monthly average precipitation and monthly actual evapotranspiration, they were calculated from the time series of monthly rainfall and temperature values measured in 28 termopluviometric stations in the entire area (Figure 2.8).

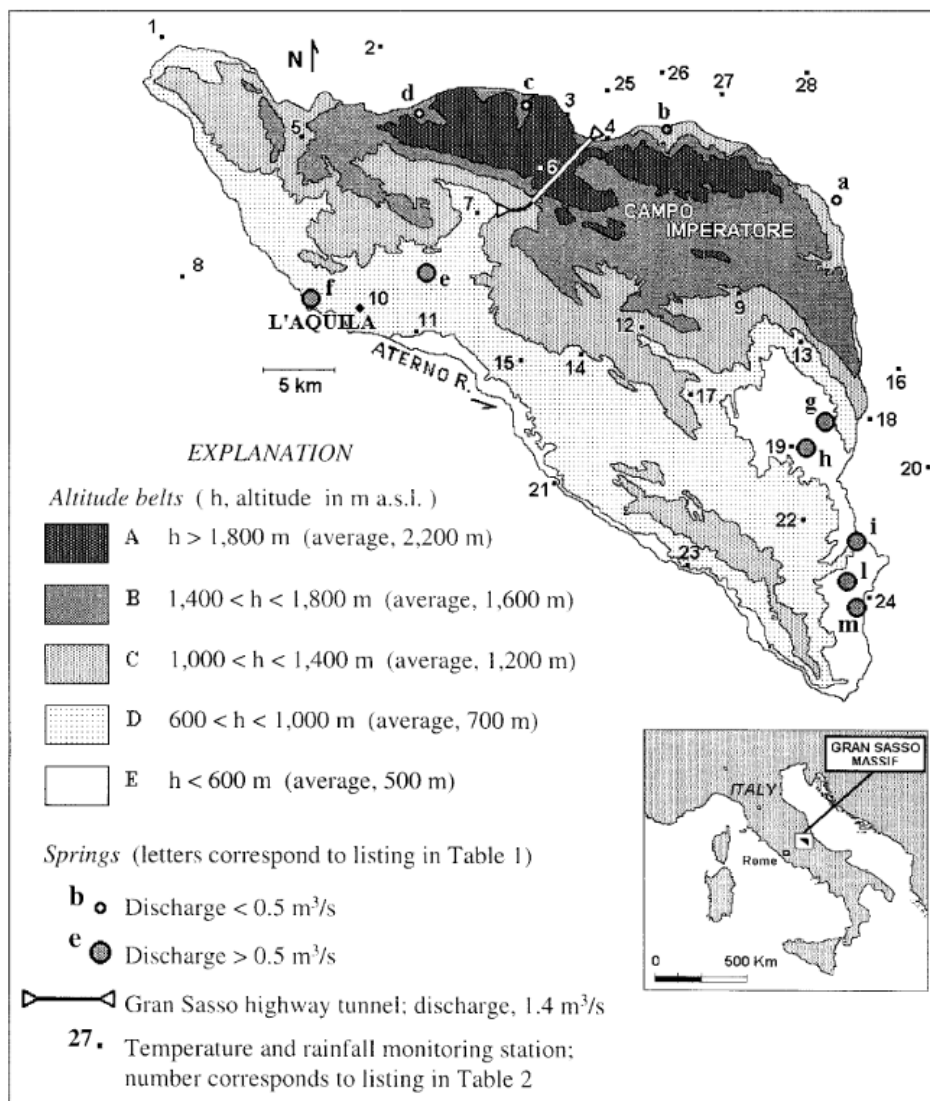


Figure 2.8 Location of temperature and precipitation stations, altitude belts, and main springs [Scozzafava, 2001].

Preliminary Water Budget

The Gran Sasso average rainfall is 945 mm/year and average monthly temperatures range from -4 to 22 °C (Scozzafava, 2001), on the basis of the total massif area of about 1080 km². This area includes non-carbonate outcrops (as Campo Imperatore basin) and on the southern side, part of the Sirente Mt. aquifer, which is feeding the Capo Pescara Spring. As explained before, a realistic water budget of the Gran Sasso aquifer cannot include the Capo Pescara spring and its recharge area, because attributed to the Sirente Mt. Aquifer.

Considering the whole area (1080 km²), the computed annual average net infiltration is 506 mm/year, i.e., about 53% of annual average rainfall. These values are estimated on the basis of precipitation and temperature data recorded for a period of about 40 years (1950–1990) (Scozzafava, 2001). The distribution of rainfall over the Gran Sasso Massif was determined by using the isohyet method rather than the topohyet method.

Because the Gran Sasso is a karstic, high-altitude area, its monthly water budgets should take into account runoff in endorheic areas and winter snowfall. Both of these parameters impact the areal distribution and amount of aquifer recharge over time. In endorheic karstic areas, runoff also contributes to net infiltration and recharge. Water budgets should take into account the fact that the water in solid form, which accumulates in winter months, is available again in liquid form during snow-melting months, and that it will add to rainfall amounts as available moisture (Scozzafava, 2001). Seasonal recharge is mainly due to snowmelt that contributes more recharge than rainfall. The water from snowmelt contributes to net infiltration and runoff in a way that is different from the same amount of water derived directly from rainfall. In areas with a thick snow cover, melting is a long process for the snow cover may persist until summer. In these circumstances, runoff concentrated below the snow cover evolves under temperature and humidity conditions that are very different from temperature and humidity conditions without snow cover. For these reasons, in the investigated area, the detailed analysis of temperature, rainfall and snow data (in terms of thickness variation of snowpack) and that of effective rainfall, have allowed to obtain relevant considerations on the meteoric inflows and its relations with the variability of the groundwater regime. Water budgets should take into account the fact that the water in solid form, which accumulates in winter months, is available again in liquid form during snow-melting months, and that it will add to rainfall amounts in the calculation of the water budget. In conclusion, the analysis of the infiltration has been based on the temperature, rainfall and snow data. The snowfall has been taking into consideration for the snowmelt, referring to some indications, like:

- Cold months are defined as the months with an average temperature <0 °C
- The snowfall months are assumed to be December, January, February, and March;
- The thawing months are defined as the first spring months with an average temperature >0 °C
- The snow-thawing months, in general, are April, May, and June. In these months, precipitation is assumed to be only rain.
- In cold months, the values of potential evapotranspiration, actual evapotranspiration, runoff, and net infiltration are zero. Precipitation is assumed to be zero only for the monthly water budget, because it is in solid form.

2.3. Discussion and Conclusion

- The Apennine carbonate aquifers, like the Gran Sasso aquifer, represent systems characterized by boundaries having zero flow generally made up of important tectonic elements (direct faults, and thrust). Thanks to quantitative hydrogeology methodology it is possible to hypothesize a conceptual model of groundwater flow.

Preliminary Water Budget

- On the basis of the previous hydrogeological data of the Gran Sasso aquifer, outlined by the researches carried out up to the 1980s, and using information from the hydrogeological balance, determined by measuring the flow rate of the springs and the discharge of the rivers, is possible to assess the amount of groundwater resources in the Gran Sasso massif.
- Boni et al. (1986) proposed a method of "direct" evaluation of the effective infiltration parameter which, starting from the flow rate supplied by the springs, goes back to the evaluation of the quantity of water that infiltrates in the carbonate aquifer, after having outlined the limits of the feeding areas on the basis of an accurate geological-structural analysis of the territory. The method of "direct" assessment of effective infiltration is therefore based on the principle that the amount of water that on average emerges from the aquifer is the same as the amount that on average penetrates it on an annual basis. Note the flow rate of the springs can be traced back to the value of effective infiltration expressed in millimeters/year.
- Using the direct method to determine the water budget, an estimation of a total spring mean discharge of about than $18 \text{ m}^3/\text{s}$ has been considered. By this way, the carbonate outcrops of the Gran Sasso aquifer (about 700 km^2 wide) result to be recharged by a net infiltration of over $800 \text{ mm}/\text{y}$ (Boni et al., 1986), with respect to an annual average rainfall of approximately $1200 \text{ mm}/\text{y}$.

Alternatively, to assess this hydrogeological parameter, "indirect" methods based on the calculation of effective rainfall are generally used, which implies a good knowledge of rainfall and a reliable assessment of evapotranspiration, in different hydrogeological and climatic environments. Given the quality of the data available for the assessment of effective rainfall, this type of approach is frequently considered unsuitable for the hydrogeological structures of Central Italy. Nevertheless, the approach to the hydrogeological balance of the Gran Sasso through methods codified in the literature (Thorntwaite & Mather, 1957), appropriately modified, has been addressed in Scozzafava & Tallini (2001). This methodology to determine the effective infiltration of the Gran Sasso (Central Apennines) carbonate massif, provides for the application of the Thorntwaite method (Thorntwaite & Mather, 1957) modified by integrating it with the use of the CN (curve-number) parameter of the US Soil Conservation Service (USDA- SCS, 1986). This approach also considers additional parameters, such as the analysis of the territory, the time and thickness of the snowpack and the determination of the distribution of the endorheic areas. Scozzafava and Tallini considered for their method, an area of approximately 1.080 km^2 wide, unlike Boni et al. (1986) who considered an area of 700 km^2 . The main differences in the area evaluation are due to the inclusion in the Scozzafava and Tallini analysis of: a) Campo Imperatore endorheic basin, about 75 km^2 ; b) part of the Sirente Mt. aquifer, for about 250 km^2 . The final product is the spatial distribution of effective infiltration. According to this study, the results of the Gran Sasso water-budget analysis, obtained from the modified Thorntwaite method integrated with the CN method, are considered to be satisfactory. The computed inflows ($17.3 \text{ m}^3/\text{s}$) and the measured outflows ($17.4 \text{ m}^3/\text{s}$) are very similar.

The results of the Gran Sasso water-budget analysis, obtained from the modified Thorntwaite method integrated with the CN method, have shown that more than half of the groundwater system has an annual recharge of lower than $400 \text{ mm}/\text{year}$. The endorheic basin of Campo Imperatore is very relevant for the recharge of the regional karstic aquifer (Scozzafava, 2001). This tectonic-karst basin, inside the Gran Sasso aquifer, has an endorheic morphology and is a preferential recharge area, also due to high rainfall amount. The combination of intense rainfall with endorheic morphology gives rise to concentrated infiltration phenomena, where an important role is played by the level of fracturing, by the presence of vegetable covers and by the characteristics and thickness of the soil. Here, net infiltration values exceed $500 \text{ mm}/\text{year}$, with peaks of $850 \text{ mm}/\text{year}$ (Figure 2.9). Furthermore, as many as eight land units lie at higher altitudes, where net infiltration can exceed $1,500 \text{ mm}/\text{year}$ (with peaks above $2,000 \text{ mm}/\text{year}$). By contrast, lower net infiltration values (less than $200 \text{ mm}/\text{year}$) occur in the

Preliminary Water Budget

Tirino River valley. The differences in net infiltration within the area are mostly related to the distribution of monthly and annual isohyets, but the diversity of soils and variability of CN also affect these values. The Gran Sasso karst massif average rainfall is 945 mm/year and (Scozzafava, 2001), meanwhile, the annual average net infiltration is 506 mm/year, i.e., about 53% of annual average rainfall.

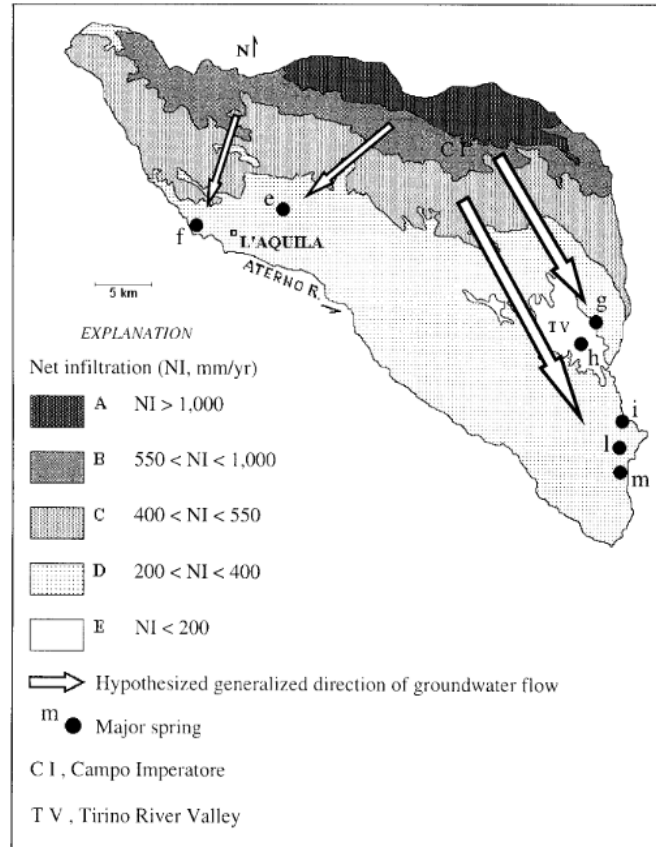


Figure 2.9: Distribution of average annual net infiltration in the Gran Sasso Massif, showing hypothesized generalized directions of groundwater flow [Scozzafava, 2001].

By the two different types of approaches for the calculation of the water budget, a significant difference has been found (Table 2.3). The values of the considered factors are difficult to compare, mainly due to the different extent of the area of interest. The main differences in the water budget is related to the role of Campo Imperatore endorheic basin (about 75 km²), where carbonate rocks are not outcropping. The runoff and snowmelt in this area directly contribute to infiltration towards groundwater, as testified by the drainage inside the highway tunnels. In addition, the southernmost area considered by Scozzafava and Tallini is dealing with Sirente Mt. Aquifer, and it has the lower infiltration values (<400 mm/y). Consequently, the real infiltration values calculated by Scozzafava and Tallini for the sole portion of the Gran Sasso aquifer, is higher than the mean value.

It can be concluded that the existing water budgets of the Gran Sasso aquifer constitute a relevant good basis of knowledge, but they need to be improved by collecting additional information (both in recharge and discharge parameters) to obtain an updated and detailed water budget useful for the goals of the KARMA project. For this aim, new monitoring activities and instruments will be carried out in the further periods in the Gran Sasso area.

Table 2.3: Description of the two different methods to obtain water budget and their parameters

| | DIRECT METHOD (Boni et al., 1986) | INDIRECT METHOD (Scozzafava & Tallini, 2001) |
|---------------------|---|--|
| Discharge springs | 18 m ³ /s | 17.4 m ³ /s |
| Average rainfall | 1200 mm/y | 945 mm/y |
| Recharge area | About 700 km ² | 1080 km ² |
| | | (including non-carbonate outcrops and part of the Sirente Mt. aquifer) |
| Net Infiltration | 800 mm/y | 506 mm/y |
| | (-66%) | (-53%) |
| ETP | About 30% | About 40% |
| Runoff | Less than 5% | About 10% |
| Snow melting months | | March-June |

2.4. References

- Accordi, G., F. Carbone, G. Civitelli, L. Corda, D. de Rita, D. Esu, R. Funicello, T. Kotsakis, G. Mariotti, and A. Sposato (1998). Note illustrative alla Carta delle litofacies del Lazio-Abruzzo ed aree limitrofe. Quaderni Ricerca Scientifica 114, N. 5.
- Adinolfi Falcone R., Falgiani A., Marco Petitta M. and Marco Tallini (2006). Characteristics of the Gran Sasso INFN laboratory groundwater (inferred from 1996-1998 spot sampling data) to fine-tune the conceptual model of water-rock interaction in carbonate aquifers
- Adinolfi Falcone, R., Falgiani, A., Parisse, B., Petitta, M., Spizzico, M., & Tallini, M. (2008). Chemical and isotopic ($\delta^{18}O\%$, $\delta^2H\%$, $\delta^{13}C\%$, ^{222}Rn) multi-tracing for groundwater conceptual model of carbonate aquifer (Gran Sasso INFN underground laboratory - central Italy). *Journal of Hydrology*, 357(3–4), 368–388.
- Amoruso, A., Crescentini, L., Petitta, M., & Tallini, M. (2012). Parsimonious recharge/discharge modeling in carbonate fractured aquifers: The groundwater flow in the Gran Sasso aquifer (Central Italy). *Journal of Hydrology*, 476, 136–146.
- Boni C., Bono P., Capelli G. (1986). Schema idrogeologico dell'Italia centrale. *Mem. Soc. Geol. It.*, 35, 991-1012, 2 tav., Roma.
- Barbieri, M., Boschetti, T., Petitta, M., & Tallini, M. (2005). Stable isotope (2H , ^{18}O and $^{87}Sr/^{86}Sr$) and hydrochemistry monitoring for groundwater hydrodynamics analysis in a karst aquifer (Gran Sasso, Central Italy). *Applied Geochemistry*, 20(11), 2063–2081.
- Celico, P., Gonfiantini, R., Koizumi, M., & Mangano, F. (1983). Environmental isotope studies of limestone aquifers in central Italy. *Isotope Hydrology*, 173-192.
- De Luca, G., Di Carlo, G., & Tallini, M. (2016). Hydraulic pressure variations of groundwater in the Gran Sasso underground laboratory during the Amatrice earthquake of August 24, 2016. *An Geop*, 59, 8–13.
- Dragoni, W. (1998). Some considerations on climatic changes, water resources and water needs in the Italian region south of 43 N. In *Water, environment, and society in times of climatic change* (pp. 241-271). Springer, Dordrecht.
- Massoli Novelli, R., Petitta, M., 1997. Hydrogeological impact of the Gran Sasso tunnels (Abruzzi, Italy). *Engineering Geology and the Environment*, vol. 3. Rotterdam, Balkema, pp. 2787–2792

- Massoli Novelli, R., Petitta, M., Salvati, R., 1999. Monitoring and protection of groundwater resources: Capo Pescara karst springs (Central Italy). XXIX Congress of International Association of Hydrogeologists
- Monjoie, A., 1980. Pr vision et contr le des caract ristiques hydrog ologiques dans les tunnels du Gran Sasso (Appenin, Italie). Livre Jubilaire, L. Calembert, Ed. Thone, Li ge
- Petitta, M., & Tallini, M. (2002). Idrodinamica sotterranea del massiccio del Gran Sasso (Abruzzo): Nuove indagini idrologiche, idrogeologiche e idrochimiche (1994-2001). *Boll Soc Geol It* 121, 343–363.
- Petitta, M., & Tallini, M. (2003). Groundwater Resources and Human Impacts in a Quaternary Intramontane Basin (L'Aquila Plain, Central Italy). *Water International*, 28(1), 57–69.
- Scozzafava, M., & Tallini, M. (2001). Net infiltration in the Gran Sasso Massif of central Italy using the Thornthwaite water budget and curve-number method. *Hydrogeology Journal*, 9(5), 461–475.
- Stoch, F., Fiasca, B., Di Lorenzo, T., Porfirio, S., Petitta, M., M.P. Galassi, D. (2015). Exploring copepod distribution patterns at three nested spatial scales in a spring system: habitat partitioning and potential for hydrological bioindication.
- Tallini, M., Petitta, M., Ranalli, D., 2000. Caratterizzazione chimico-fisica e idrologica delle acque sotterranee del massiccio del Gran Sasso d'Italia (Italia centrale): Analisi statistica dei dati esistenti. Dipartimento di Ingegneria delle Strutture, delle Acque e del Terreno, Aquila. DISAT
- Tallini, M., Parisse, B., Petitta, M., & Spizzico, M. (2013). Long-term spatio-temporal hydrochemical and ²²²Rn tracing to investigate groundwater flow and water–rock interaction in the Gran Sasso (central Italy) carbonate aquifer. *Hydrogeology Journal*, 21(7), 1447–1467.
- Toth, J. (1963). A theoretical analysis of groundwater flow in small drainage basins. *Journal of geophysical research*, 68(16), 4795-4812.
- White, W. B. (2003). Conceptual models for karstic aquifers. *Karst modeling: special publication 5*, The Karst Waters Institute, Charles Town, WVA.

3. The Qachqouch aquifer (Case study Lebanon)

3.1 Field site description – river and spring

Qachqouch Spring (Figure 3.1) is located within the Nahr el Kalb Catchment, and originates from the Jurassic karst aquifer at about 64 meters above sea level. During low flow periods, the spring is used to complement the water deficit in the capital city Beirut and surrounding areas. Its total yearly discharge reaches 35-55 Mm³ based on high resolution monitoring of the spring (2014-2019; *Dubois et al., submitted, Dubois, 2017*). Flow maxima reach a value of 10 m³/s for a short period of time following flood events; it is about 2 m³/s during high flow periods and 0.2 m³/s during recession periods.

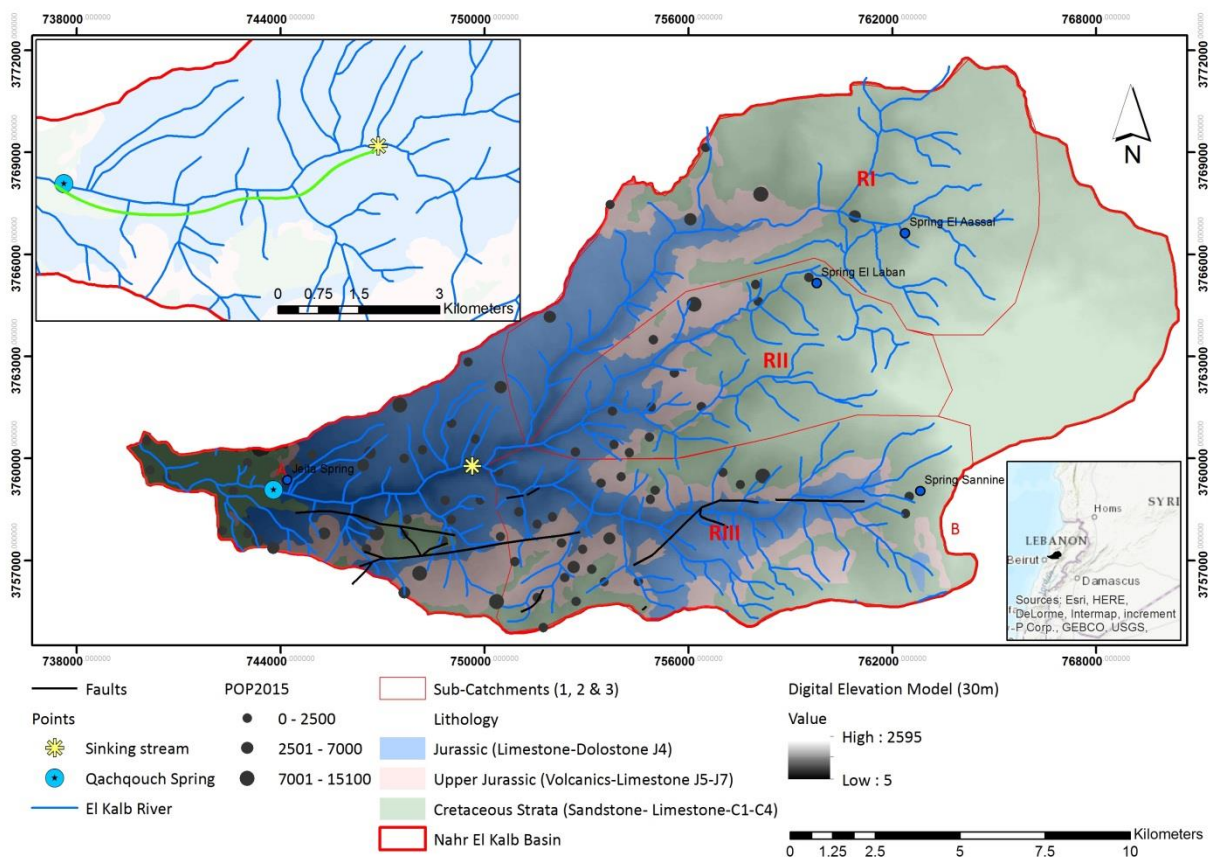


Figure 3.1 Investigated Spring (Qachqouch) and River (Nahr el Kalb) watersheds showing the relationship between a sinking stream on the River and the spring (Aoun, 2019)

The lithology of the surface water and groundwater catchments mostly consists of Jurassic karstified limestone to dolomitic limestone (in the higher plateaus) grading into more massive micritic limestone in the lower portion of the catchment. Formations of middle cretaceous age are exposed on the upper parts of the catchment (Figure 3.3, Dubois, 2017).

The Qachqouch spring is a karst spring characterized by a duality of flow in a low permeability matrix and high permeability phreatic conduit system (Dubois, 2017). It is highly reactive to rain events with recession coefficient ranging between 0.005 and 0.1 depending on the event responses (Dubois, 2017). About 3% of the River infiltrates into the Qachqouch spring based on multiple tracer test experiments conducted in the River during different flow periods. The estimated transport velocities vary between 0.02 and 0.05 m/s (Aoun, 2019).

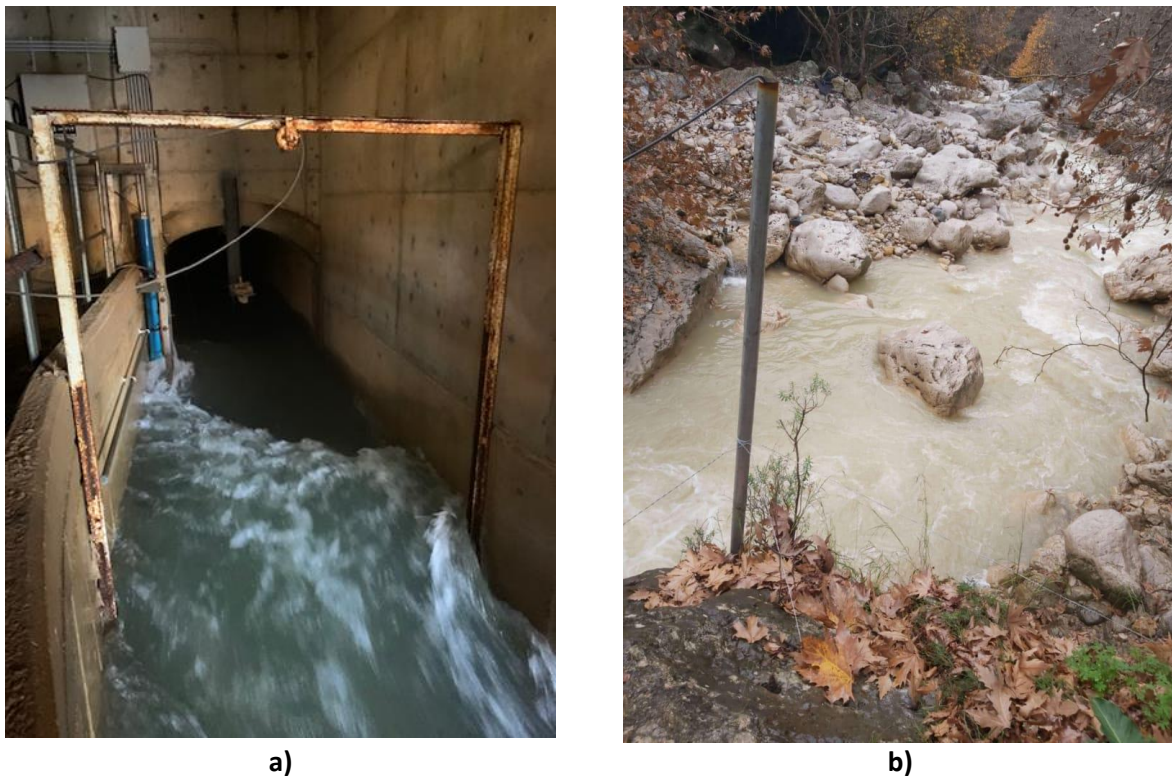


Figure 3.2 a) Qachqouch spring during high flow (picture taken February 2020); b) Nahr el Kalb River- a pressure transducer was installed in November 2019 (picture taken January 2020)

The total yearly precipitation is estimated from two stations deployed over the surface and groundwater catchment to about 950-1500 mm on average (2014-todate; local high-resolution monitoring). The latter includes the snow component contributing locally to the river in March and April of each hydrological year (Dubois 2017).

Qachqouch spring is highly polluted due to excessive waste discharge located in its urbanized catchment upstream, in addition to the input from the River through a sinking stream. Raw wastewater is either directly discharged into the river system or bottomless cesspits or overflowing in valleys, as there are no effective wastewater treatment plants (WWTPs) on the studied catchment area (Doummar and Aoun, 2018b).

Nahr El Kalb River is originating from springs in the highlands of Kesrouane area, in addition to interflow and runoff occurring shortly after rain events and snowmelt. Its catchment is about 249 km², and extends from the outlet of the River on the coast to about 22 km to the east in the Lebanese Mountains (Margane, A. & Stoeckl, L., 2013). Its southern and northern boundaries were delineated based on topography highs. The river consists of three sub-catchments (RI -Nahr El Salib; RII-Nahr el Ouadi, and RIII- Nahr Abou Mizane; Figure 3.1) joining together to form the main branch of the River (Figure 3.1). Its peak discharge reaches a maximum of 22 m³/s, with a yearly discharge volume of 80.0- 230 Mm³ (based on River measurements from 2014-2017).

Most of the River runoff is generated as a response to precipitation events between December and March, from snowmelt in the highlands (1200-2200 m above sea level) occurring between March and April of the same hydrological year. From August till October, the River flow does not exceed 0.8 m³/s at its outlet; while the three upper tributaries (RI, RII, and RIII) run dry (Doummar and Aoun, 2018b).

Preliminary Water Budget

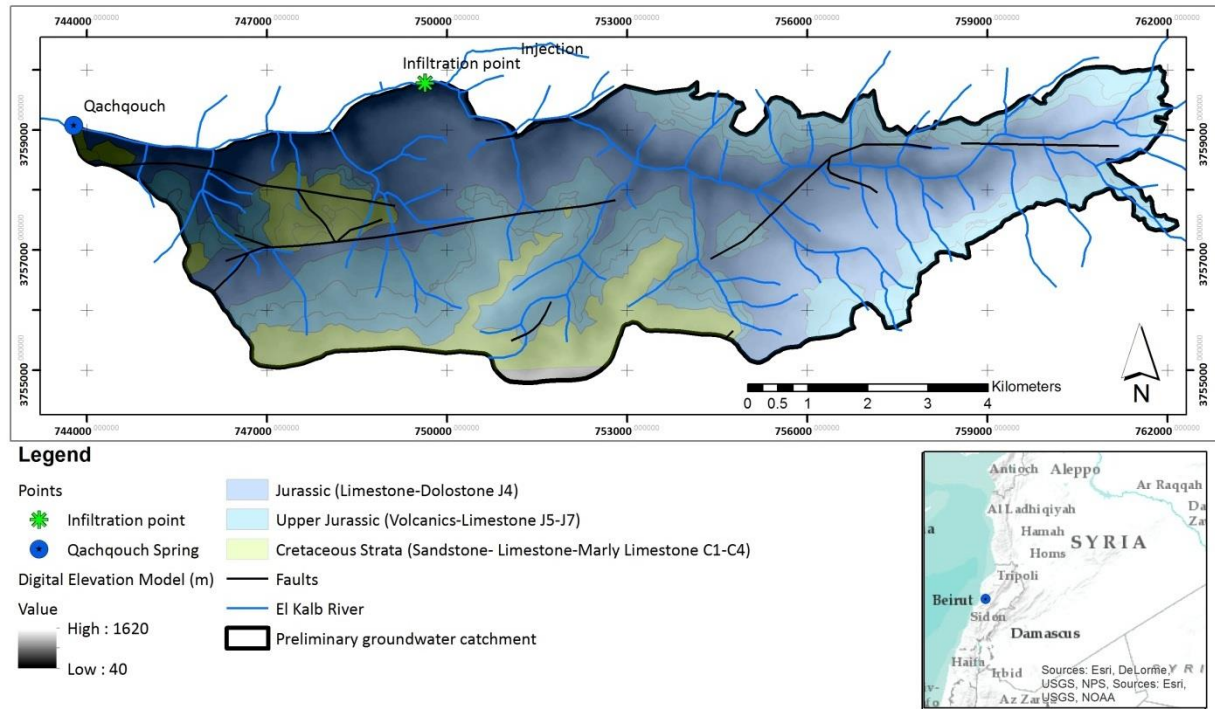


Figure 3.3 Geological map of the Qachqouch spring catchment outlined to date based on tracer experiments, geological boundaries and topography (Doummar and Aoun, 2018a)

3.2 Catchment monitoring, data collection and analysis

Data related to water balance is currently being collected on the Qachqouch catchment as follows (Table 3.1). A representation of the collected time series is shown on Figure 3.4.

Table 3.1 Collected data from the monitoring equipment, frequency and duration of monitoring.

| Data monitoring | Frequency of monitoring | Time frame |
|---|-------------------------|---------------------------|
| Precipitation and other climatic series (x2 at elevations 950 m and 1700 m) | 15- 60 min | Continuing (since 2014) |
| River time series (discharge, level, and temperature) | 1 hour | Nov, 15, 2019- continuing |
| Spring discharge (Qachqouch) | 30 min | Sept 2014- continuing |
| EC, Temp, TU, and pH | 30 min | Sept 2014- continuing |
| DO | 30 min | Sept 2018- continuing |
| Automatic sampler for grab sample analysis | Every 3 days | Nov 27, 2019- continuing |
| Isotope analysis (spring) | Every 3 days | Nov 27, 2019- continuing |
| Major Chemical analysis | occasional | - |
| Bacterial analysis (River and spring) | weekly | Mid-Jan, 2020-ongoing |

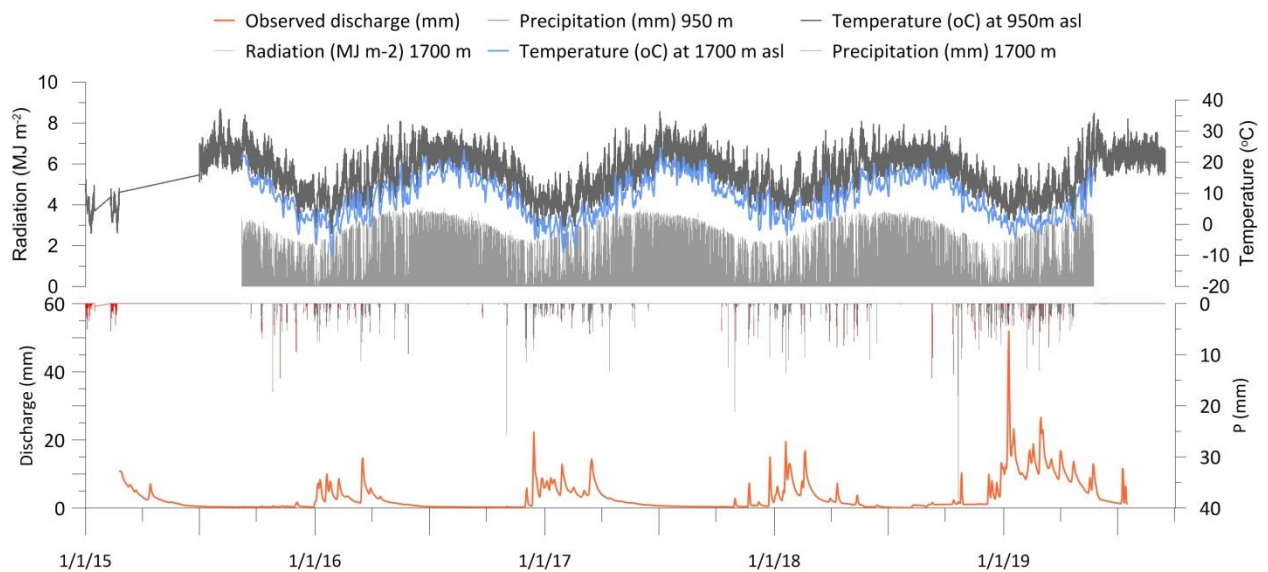


Figure 3.4 Climatic data collected from two climatic stations (at different altitudes) and spring discharge (Qachqouch) estimated from a calibration curve.

3.3 Preliminary water budget and catchment delineation

The catchment was delineated based on tracer experiments, structural boundaries and geological information. The preliminary delineated catchment is estimated to about 56 km².

The water balance was assessed based on a simple linear reservoir model (Dubois, 2017, *Dubois et al., submitted*) on data over 5 consecutive years (2014-2019). The model accounts for a limited unsaturated zone thus the likelihood of an underestimated real evapotranspiration, which accounts for a maximum of 12-30% occurring mostly during 7 to 8 months during the hydrogeological year. The area is highly karstified, thus surface runoff was neglected (Table 3.2)

Stable isotope data collected only during a four –precipitation event (in 2016) show a limited influence of snow melt during December –January of this hydrogeological year (Doummar and Aoun 2018a).

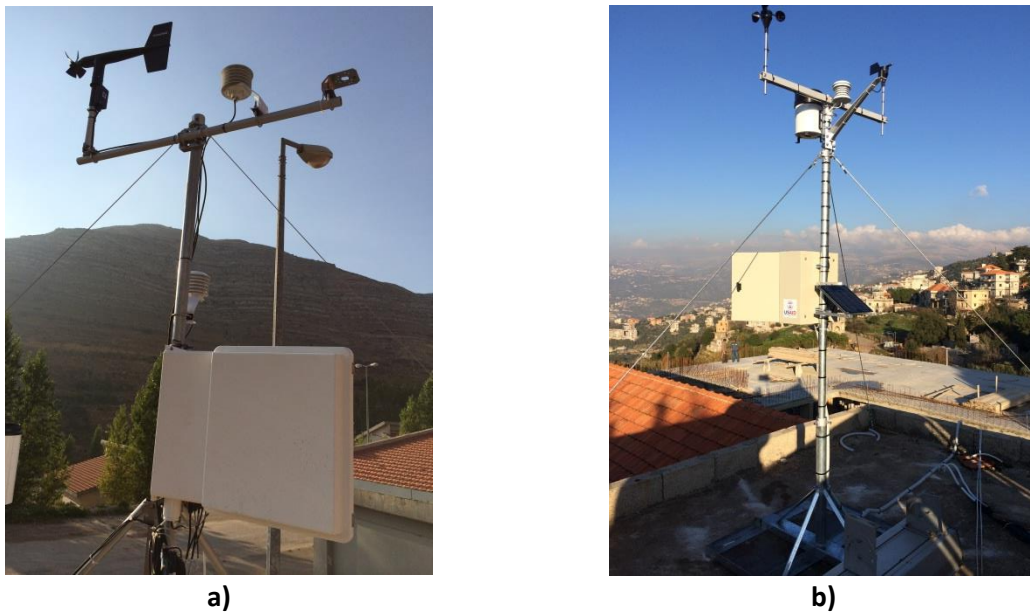


Figure 3.5 a) Climatic Station at 1700 m (above sea level; asl); b) At 950 m (asl) installed in the framework of a USAID (PEER Science supported project).

Table 3.2 Preliminary water balance assessment for the Qachqouch catchment (the spring being the only outlet).

| Total Precipitation (mm) Value at 950 m asl | Recharge Q (Qachqouch) | Real Evapotranspiration (%) |
|--|--|--------------------------------|
| 921 mm (2015-16) | 35 Mm ³ (2015-16)-652 mm (70%) | 10-30% of total budget |
| 1034 mm (2016-17) | 47 Mm ³ (2016-17)- 839 mm (81%) | |
| 1089 mm (2017-18) | 50 Mm ³ (2017-18)- 892 mm (81%) | |
| Wet year | Extreme wet year: | |
| 1800 mm (2018-19) | In processing | |

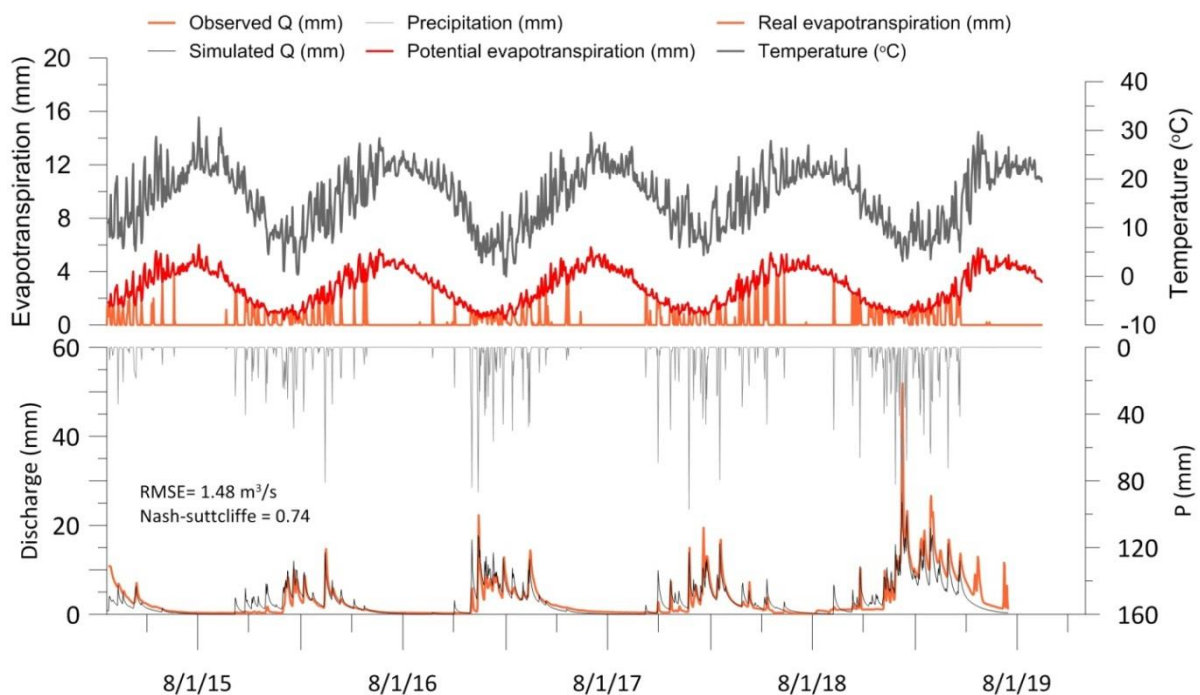


Figure 3.6 The linear reservoir model output (Mike she; DHI, 2017) for the Qachqouch spring based on which the water balance was preliminary assessed for the monitored years (2014-2019).

3.4 Current activities related to Water Balance Assessment

Current ongoing activities aim at refining the water balance and at the understanding of the flow dynamics in the Qachqouch system, especially under varying conditions (wet and dry years) as follows:

1. Discharge measurements and calibration curves (Water level and flow measurements): An update of the calibration curve of discharge-water level
2. Tracer experiments on the upper catchment (dolines and dolomite outcrops): A tracer test is scheduled mid-march (when the spring becomes accessible for the installation of equipment)
3. Advanced mapping and soil characterization: to identify and map dolines in the upper catchment and for the characterization of the soil cover in specific locations.
4. Calculation of Evapotranspiration using the modified Penman-Monteith (FAO, 1997) based on the newly acquired data set for the purpose of updating the existing model with a more developed unsaturated zone
5. A sampling of the Qachqouch spring (every 3 days) for stable isotope analysis since November 2019 will allow a better understanding of recharge during the entire hydrogeological year (potential snow influence, river input, others)

3.5 References

- Aoun, M. (2019) Occurrence and Transport of selected Micropollutants in Surface water and Groundwater under varying dynamic conditions: Application on the Qachqouch karst catchment Lebanon. Master thesis, American University of Beirut, Department of Geology, Beirut, Lebanon. 2019
- Doummar, J., Aoun, M. (2018). Occurrence of selected domestic and hospital emerging micropollutants on a rural surface water basin linked to a groundwater karst catchment, *Environmental Earth Sciences*, 77(9), 351, doi: 10.1007/s12665-018-7536-x, 2018b.
- Doummar, J., Aoun, M. (2018). Assessment of the origin and transport of four selected emerging micropollutants sucralose, Acesulfame-K, gemfibrozil, and iohexol in a karst spring during a multi-event spring response, *Journal of Contaminant Hydrology*, doi:10.1016/j.jconhyd.2018.06.003, 2018a.
- Dubois, E. (2017). Analysis of high resolution spring hydrographs and climatic data: application on the Qachqouch spring (Lebanon), Master thesis, American University of Beirut, Department of Geology, Beirut, Lebanon. [online] Available from: https://www.researchgate.net/profile/Emmanuel_Dubois5, 2017.
- Dubois, E., Doummar, J., Pistre, S., and Larocque, M. (2020): Calibration of a semi-distributed lumped karst system model and analysis of its sensitivity to climate conditions: the example of the Qachqouch karst spring (Lebanon), *Hydrol. Earth Syst. Sci. Discuss.*, <https://doi.org/10.5194/hess-2020-90>, in review, 2020.

4. The Eastern Ronda Mountains (study area in Spain)

4.1 Field site description

The study area selected for the KARMA project is Eastern Ronda Mountains, located in southern Spain (western region of Málaga province), it covers a total surface of around 110 km² and it is constituted by Sierras of Merinos-Colorado-Carrasco aquifer systems. In addition, owing to its hydrogeological features, a further karstic area of 26 km² in Sierra de Ubrique (eastern border of Cádiz province) has been included in the study area as the pilot site for developing and testing the proposed task dealing with *Early Warning Systems* (EWS). Both aquifer systems are quite representative of mountainous carbonate aquifers in Spanish Mediterranean area having highly variable recharge and limited groundwater resources.

The strategic interest of this area is directly linked to quality water supply of four villages located within the study area (Serrato, Cuevas del Becerro, Arriate and Ubrique), providing drinking water for approximately 23.000 people. Groundwater supply is performed by pumping or flow derivations in places situated close to the spring. Although to a lesser extent, other water usages are carried out in this population where economy is supported by animal breeding and agricultural activities such as olive tree plantation.

From a geological standpoint, the study area is located in the western sector of Betic Cordillera, immediately to the north of the contact between Outer and Inner zones of this alpine chain and it belongs to Penibetic (western Inner Subbetic) domain (Martín-Algarra, 1987). Sierras of Merinos, Colorado, Carrasco and Ubrique carbonate massifs are related with other structural units (Fig. 4.1) (Martín-Algarra, 2008). The stratigraphic sequence is constituted of three main groups (Cruz-Sanjulián, 1974; Martín-Algarra, 1987): clays with Triassic evaporites, Jurassic limestones (upper) and dolostones (lower), 500 meters thick and Cretaceous-Paleogene marly-limestones. Both test sites described in the first paragraph are fractured and karstified aquifer systems characterized by the same geological formations.

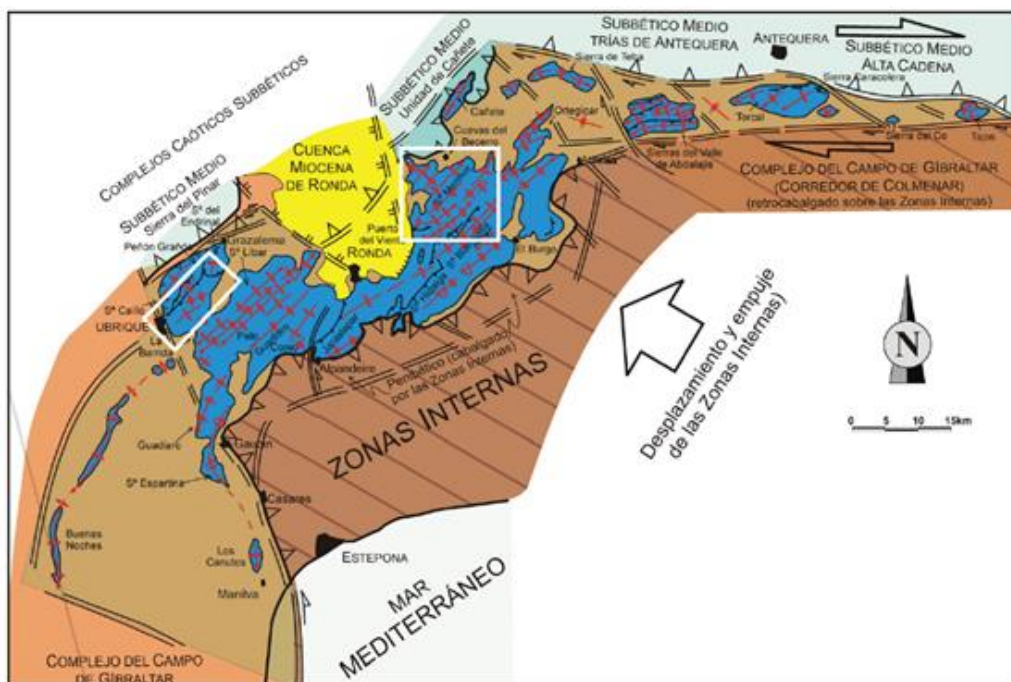


Figure 4.1 Spatial distribution of Penibetic outcrops in western Betic Cordillera in relation with other structural units. Study area is indicated within white boxes (Martín-Algarra, 2008).

Preliminary Water Budget

The **Merinos-Colorado-Carrasco** test site is located approximately 20 km to the east of the Ronda city and is composed by three Sierras of the same name aligned in direction NE-SW. This site presents outcrops of Flysch sandstones and clays (Cretaceous-lower Miocene) represented in the eastern sector (Fig. 4.2), overthrusting previously described geological formations. Discordant above all these upper Miocene calcareous sandstones are found, belonging to the sedimentary infilling of the Ronda basin, in the western part. The geological structure is constituted by box-type folds, oriented NE-SW and plunging toward NE (Martín-Algarra, 1987).

From a hydrogeological outlook, Jurassic limestones cover a large area in the test site and these (aquifer) lithologies are represented on surface, as karst exposures, or in depth, as buried aquifer segments (geological cross-sections A-A' to D-D'; Fig. 4.3). Dolomitic rocks, which comprise the lower levels of the Jurassic aquifers, can reach higher positions in the lithological sequence, and even appear on surface. Gypsum bearing formations (Triassic clays with gypsum), whose thickness is still imprecise, constitute the lower limit of the main aquifers and can uplift through faults.

Recharge takes place by the infiltration of rainwater through limestone and dolostone outcrops, while discharge is made through springs located at the borders, between the permeable carbonate rocks and the impervious layers (Cretaceous marly limestones and clays from Flysch). Hence, several outlets emerge in the middle of cretaceous rocks where Jurassic limestones are shallower (Fig. 4.2).

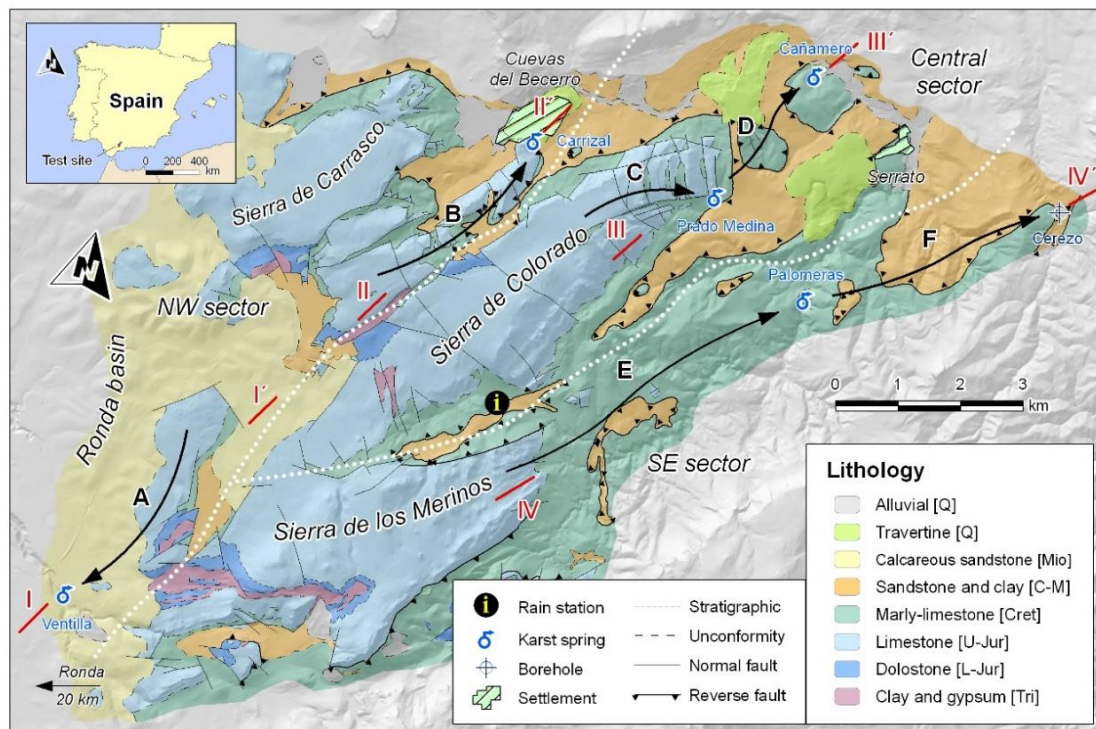


Figure 4.2 Hydrogeological setting of Merinos, Colorado y Carrasco aquifer systems (Barberá et al., 2012).

Three hydrogeological sectors have been identified in this area, on the basis of strictly geological, hydraulic and hydrochemical criteria (Fig. 2): the NW sector (Sierra de Carrasco), including the eastern part bordering with the Ronda basin, the central sector (Sierra de Colorado) and the SE sector (Sierra de los Merinos). Drainage in the **Merinos-Colorado-Carrasco** aquifer system is made in natural regime, mainly towards NE border, through the springs of Cañamero (540 m a.s.l.), Prado Medina (660 m a.s.l.), an overflow type associated with the latter), Palomeras (560 m a.s.l.) and Carrizal (740 m a.s.l.). In addition, groundwater transference toward the porous aquifer of the Ronda basin (overlying the Jurassic aquifer) exists and, the shallower (visible) discharge takes place via Ventilla spring (740 m a.s.l.).

Preliminary Water Budget

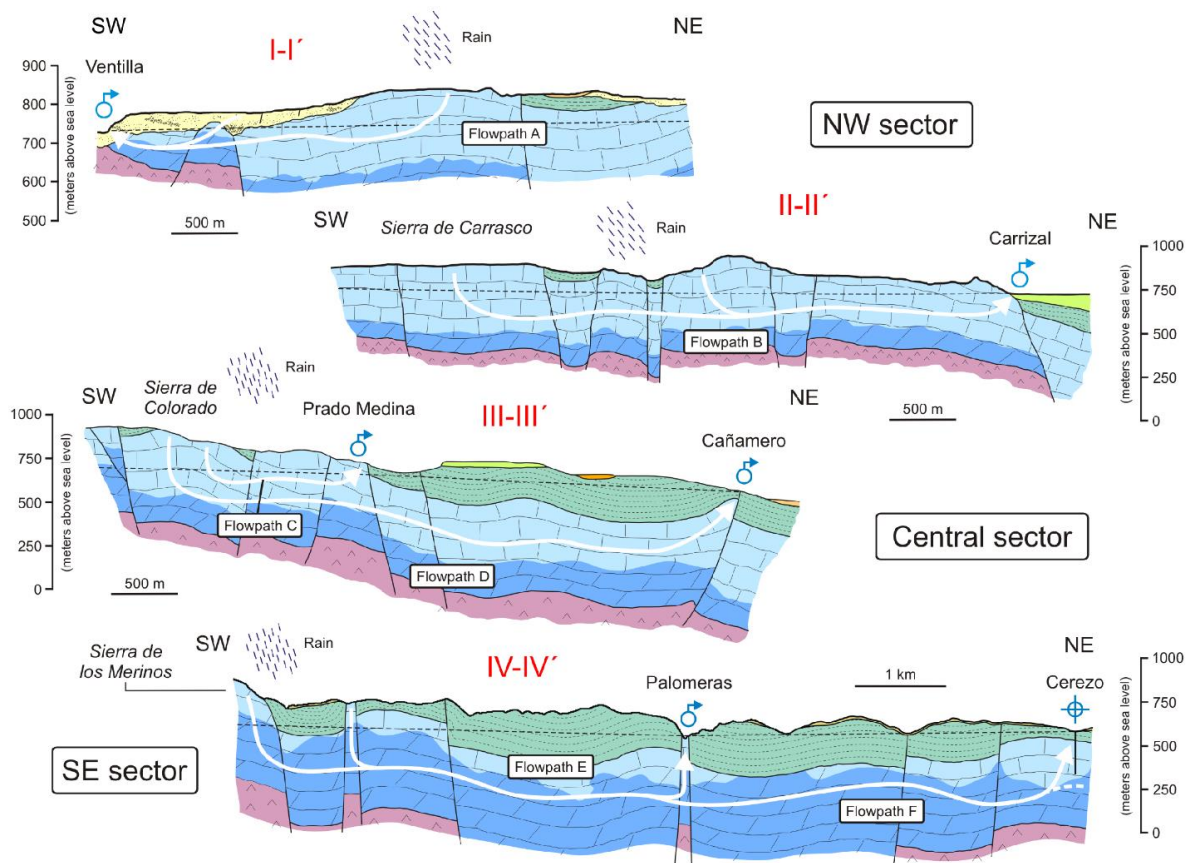


Figure 4.3 Hydrogeological scheme of the main drainage zones of Merinos, Colorado and Carrasco aquifers systems. Schemes direction is indicated on Figure 1 (Barberá et al., 2012).

Sierra de Ubrique test site is placed within Sierra de Grazalema Natural Park, in the eastern part of the Cádiz province and 35 km of distance from the main area. Aquifer formations in this area are also developed in Jurassic dolostones and limestones, resulting in highly fractured and karstified systems (Fig. 4.4) (Martín-Rodríguez et al., 2016). Geological structure is defined by NE-SW direction folds in which anticline core dolostones and limestones are found, while cretaceous marls outcrop in syncline part (geological cross-section I-I'; Fig. 4.5). In the same way that happens in Serranía de Ronda, clays and sandstones overthrust the previous geological formations in exception of some zones where Flysch materials structurally imbricate between Mesozoic rocks in the "Corredor del Boyar" (Martín-Algarra, 1987). This corridor provokes the individualization of two hydrogeological systems: one in the north (subbetic sector) and one in the south (penibetic sector), in which is included the Sierra de Ubrique (Fig. 4) (Martín-Rodríguez et al., 2016). In this case, recharge takes place mainly by the infiltration of rainwater through limestone outcrops and an allogenic recharge which enters the system through Villaluenga del Rosario shaft. Drainage in the Sierra de Ubrique aquifer system is made through the springs Nueve Caños (346 m a.s.l.), Cornicabra (349 m a.s.l.), Algarrobal (317 m a.s.l.) and Garciago (422 m a.s.l., an overflow type associated with the previous springs).

The use of artificial tracers allowed to verify hydrogeological connection between direct infiltration points and main springs as well as estimate maximum flow speed, which resulted in 183,6 m/h for Garciago spring, 128,9 m/h and 177,7 m/h for Algarrobal and Cornicabra

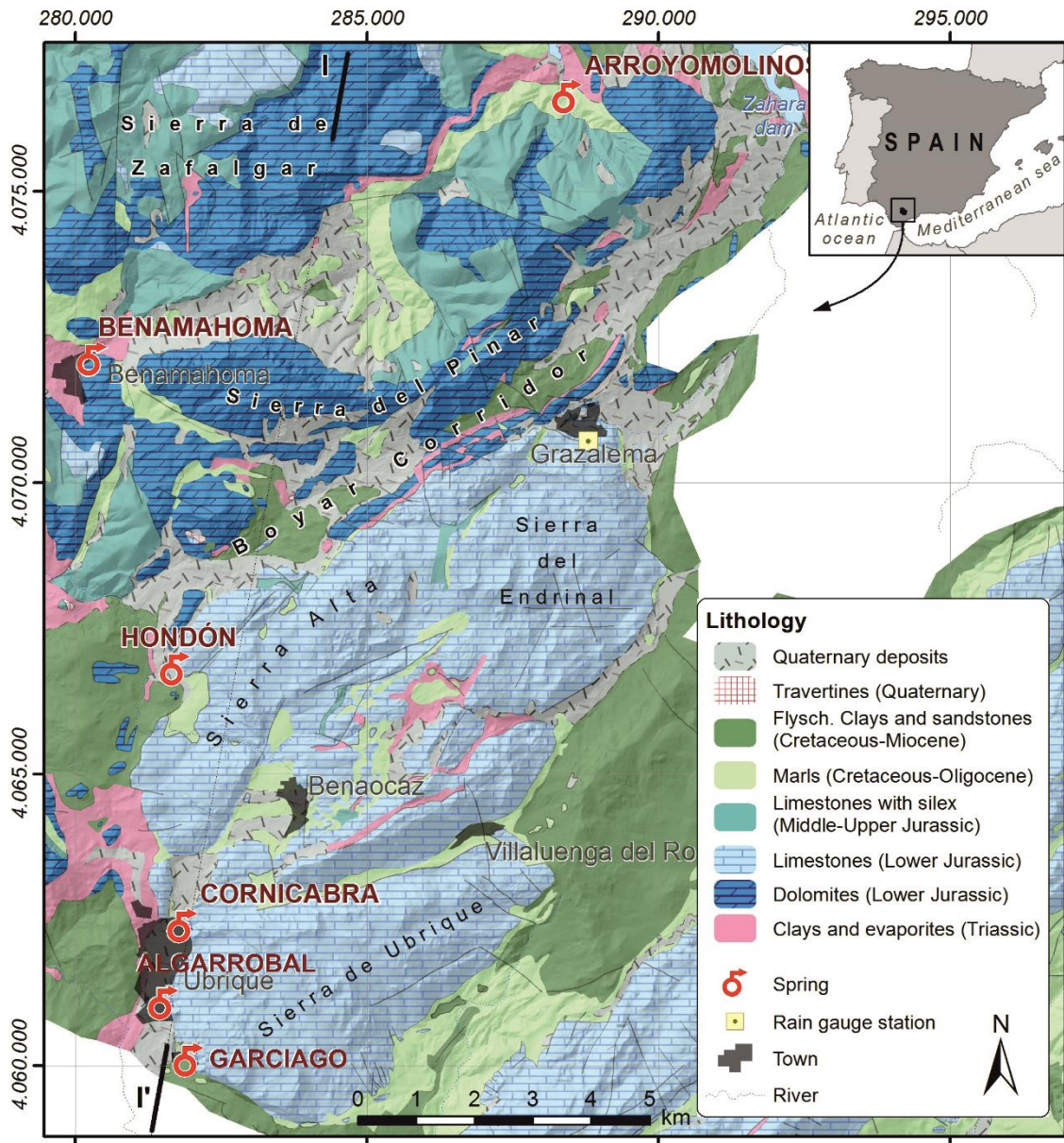


Figure 4.4 Hydrogeological setting of Sierra de Ubrique aquifer system (Sánchez et al., 2017)

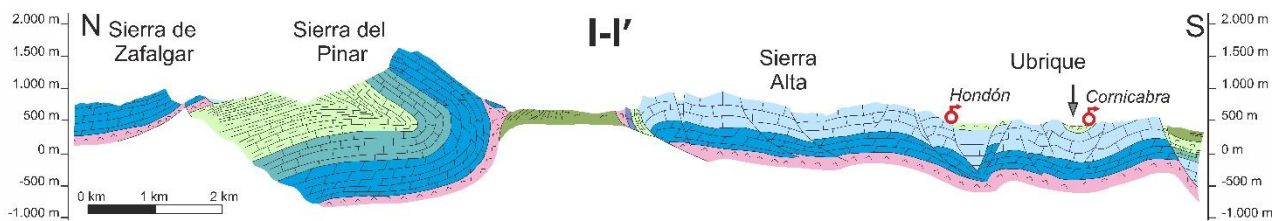


Figure 4.5 Hydrogeological cross section of the main drainage zones of Sierra de Ubrique aquifer system. Schemes direction is indicated on Figure 4 (Sánchez et al., 2017).

3.2 Preliminary water budget

The location and movement of water into and through karst drainage systems depends on the spatial and temporal distribution of recharge as rainfall (Goldscheider and Drew, 2007). In the study area, cloud fronts indicate to have Atlantic and Mediterranean origin, given the proximity of both sources of water vapour. In general, the annual distribution of precipitation presents a marked seasonal pattern. Thus, the first rainfall normally takes place in the autumn, at the beginning of the hydrological year. This is often in the form of intense storms from the Mediterranean, featuring heavy precipitation. The winter is characterised by the arrival of cloud fronts, mainly from the Atlantic, which account for most of the annual precipitation. During the rest of the year, rainfall is scarce to non-existent, particularly in the summer (Barberá et al., 2012).

In karst drainage systems a simple water balance can be described by:

$$\Delta S = P - (Q_{out} + ET)$$

where P is the precipitation (input) into the drainage system, Q_{out} is the discharge leaving, ET is evapotranspiration, and ΔS represents changes in storage, which over longer timescales are often assumed to be negligible (Goldscheider and Drew, 2007).

Different methods were used in order to estimate the different components of the previous equation, most of them based on information from rain and evapotranspiration data, as the difference between them allows obtaining effective rainfall values. Depending on ground features, such as slope or hydraulic conductivity, the effective rainfall could generate infiltration or surface runoff. In both of test sites main inputs came from net infiltration from rainfall over carbonate outcrops and, in Sierra de Ubrique site, also from infiltration of surface flows. Surface runoff that could be generated in carbonate outcrops has not been taken into account for calculating the water budget due to the high hydraulic conductivity of Jurassic limestones and sandstones, the low slope of the ground (< 10%) and the abundance of exokarstic landforms. Regarding surface runoff, it mainly generates over Cretaceous marly and marly limestones and Flysch clay formations. Calculations for both test sites have been realized from rainfall and air temperature monthly data through the use of TRASERO v.2.1.0 code (Padilla et al., 2013).

In **Merinos-Colorado-Carrasco** test site recharge area is mainly composed by surfaces located at high altitude (700-900 m.a.s.l.) and mean annual precipitation has been estimated to 733 mm (31,7 hm³/year) by isohyet planimetry (Fig. 4.6) (Barberá. 2014). This aquifer system is highly karstified and carbonate formations constitute preferential zones for direct infiltration which correspond to karren fields, dolines and uvalas.

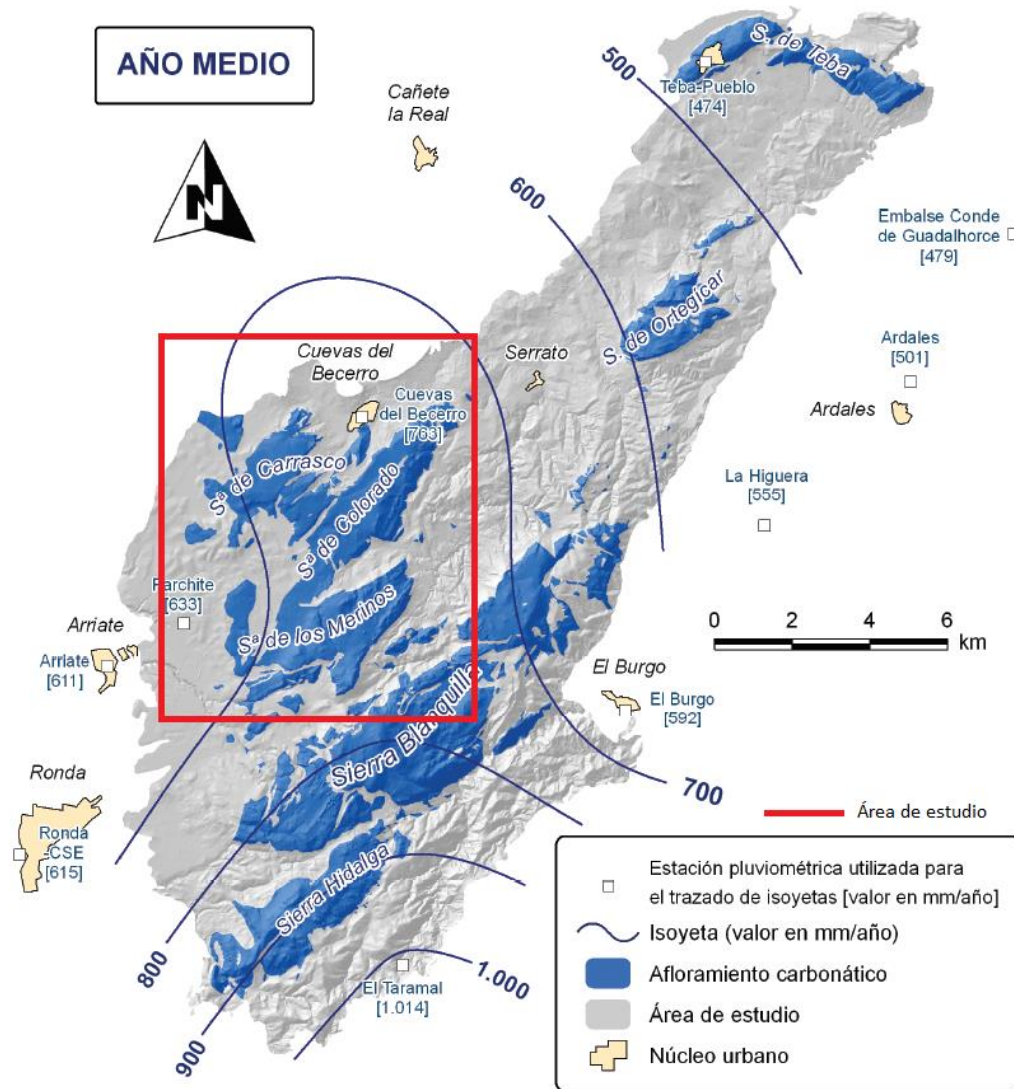


Figure 4.6 Isohyet map corresponding to mean year on the historical period 1964/65-2009/10 (Barberá, 2014).

For the analysis of spatial data, only Jurassic limestones and dolostones have been considered in order to compare recharge rates between different methods or empirical formulas. Historical records (1964/65-2009/10) have been used for this water budget (Barberá, 2014). After an intercomparative analysis between the effective rainfall results obtained with Thornthwaite (1948), Kessler (1967) and APLIS (Andreo et al., 2004 y 2008; Marín, 2009), recharge rate has been estimated using this last method as it introduces a higher number of parameters and gives more accurate results (Fig. 4.7).

The mathematic expression that allows estimating the recharge rate is:

$$R = [(A + P + 3 \cdot L + 2 \cdot I + S) / 0,9] \cdot Fh$$

where **A**, **P**, **L**, **I** y **S** refers to each variable: altitude, slope, lithology, infiltration circumstances and soil according to the table, and **Fh** is the correction factor for recharge (**R**) (Tab. 4.1).

Preliminary Water Budget

Table 4.1 Considered scores for each variable on APLIS method (IGME-GHUMA, 2003; Andreo et al., 2008) modified by Marín (2009).

| Altitud (A) | Puntuación | Pendiente (P) | Puntuación | Litología (L) | Puntuación |
|----------------|------------|---------------|------------|---|------------|
| ≤ 300 m s.n.m. | 1 | ≤ 3 % | 10 | Calizas y dolomías karstificadas | 10-9 |
| 300-600 | 2 | 3-5 | 9 | Mármoles fracturados algo karstificados | 8-7 |
| 600-900 | 3 | 5-10 | 8 | Calizas y dolomías fisuradas | 6-5 |
| 900-1.200 | 4 | 10-15 | 7 | Arenas, gravas y coluviones | 4 |
| 1.200-1.500 | 5 | 15-20 | 6 | Brechas y conglomerados | 3 |
| 1.500-1.800 | 6 | 20-30 | 5 | Rocas plutónicas y metamórficas | 2 |
| 1.800-2.100 | 7 | 30-45 | 4 | Esquistos, pizarras, limos, arcillas | 1 |
| 2.100-2.400 | 8 | 46-65 | 3 | | |
| 2.400-2.700 | 9 | 65-100 | 2 | | |
| > 2.700 | | > 100 | 1 | | |

| Suelo (S) | Puntuación | Infiltración-absorción preferencial (I) | Puntuación |
|---|------------|---|------------|
| Litosoles | 10 | Alto desarrollo de las formas de infiltración preferencial | 10 |
| Arenosoles álbicos y xerosoles cálcicos | 9 | Desarrollo moderado de las formas de infiltración preferencial | 5 |
| Regosoles calcáreos y fluvisoles | 8 | Escaso desarrollo o ausencia de las formas de infiltración preferencial | 1 |
| Regosoles eútricos, dístricos y solonchaks | 7 | | |
| Cambisoles cálcicos | 6 | | |
| Cambisoles eútricos | 5 | | |
| Histosoles eútricos, luvisoles órticos y cálcicos | 4 | | |
| Luvisoles crómicos | 3 | | |
| Planosoles | 2 | | |
| Vertisoles crómicos | 1 | | |

| Tasa de recarga (R) | Puntuación | Características hidrogeológicas de los materiales que afloran (F _h) | Puntuación |
|---------------------|------------|---|------------|
| ≤ 20 % (P) | Muy baja | Características acuíferas | 1 |
| 20-40 | Baja | Otros | 0,1 |
| 40-60 | Moderada | | |
| 60-80 | Alta | | |
| > 80 | Muy alta | | |

Through the application of this approach, APLIS showed up a mean recharge rate for Sierras of Merinos, Colorado and Carrasco of 56,71 % with a diverse spatial distribution due mainly to altitude differences. As annual mean precipitation (P) for the historical period is 31,7 hm³/year, a value of effective runoff (PU) of 17,9 hm³/year is therefore estimated (Fig. 4.8). The following equations have been applied for water budget calculations:

$$PU = P \times APLIS_{\text{recharge rate}}$$

$$ETR = P - PU$$

As there is not the same temporal resolution for discharge data than for climatic variables, renewable water resources in this aquifer system must be inferred from previous studies and values given by different authors (Tab. 4.2).

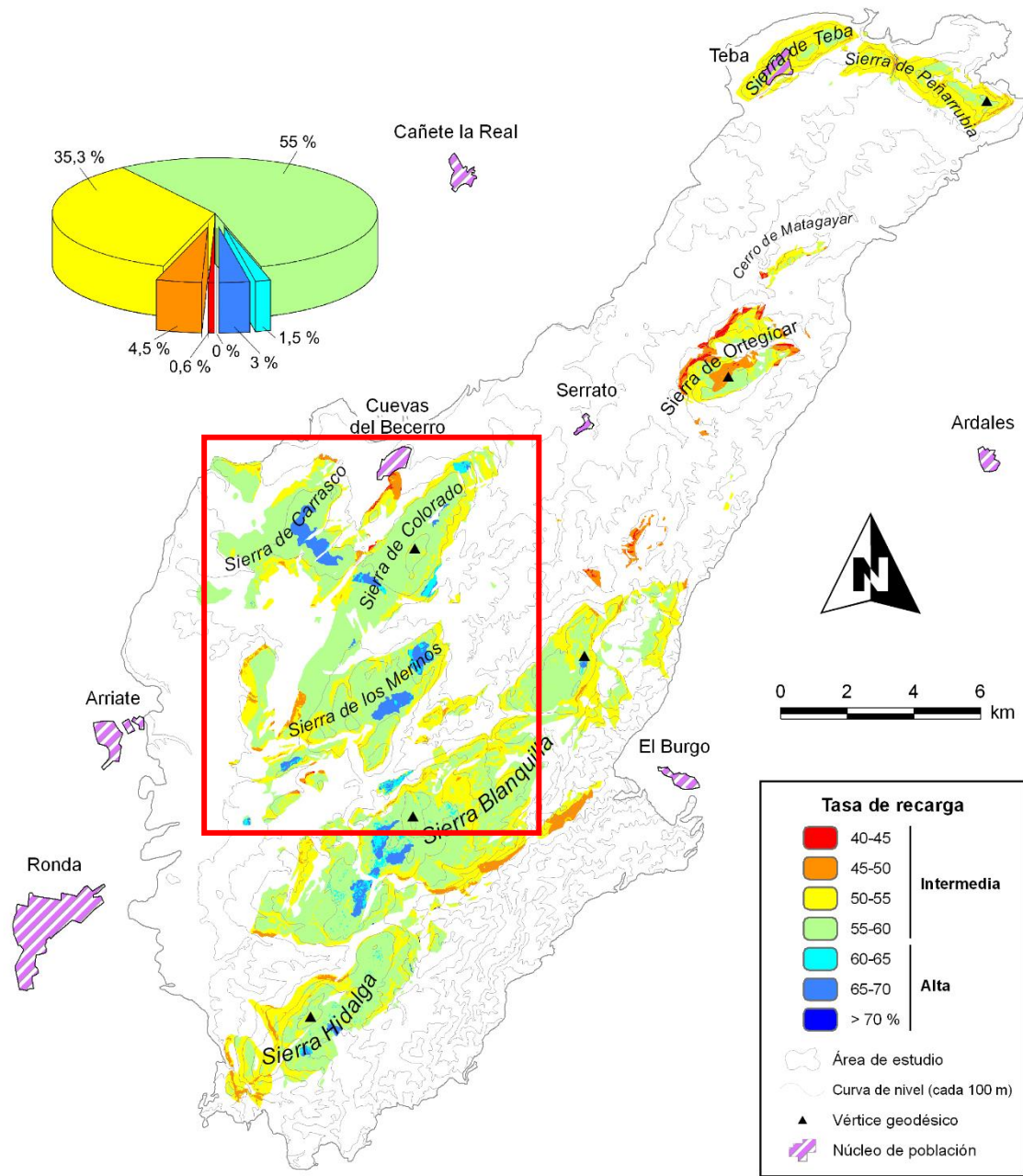


Figure 4.7 Recharge rate distribution obtained through the application of APLIS method for Merinos-Colorado-Carrasco test site (on red box) (modified from Barberá, 2014).

Table 4.2 Mean renewable resources ($hm^3/year$) at Merinos-Colorado-Carrasco test site estimated on previous studies (modified from Barberá, 2014).

| | Fernández (1980) | IGME (1983) | DPM (1988) | Barberá (2014) |
|--|---------------------|----------------|---------------|-------------------|
| Sierras de Merinos, Colorado y Carrasco | 24,3 | 17,99 | 17 | 17,96 |

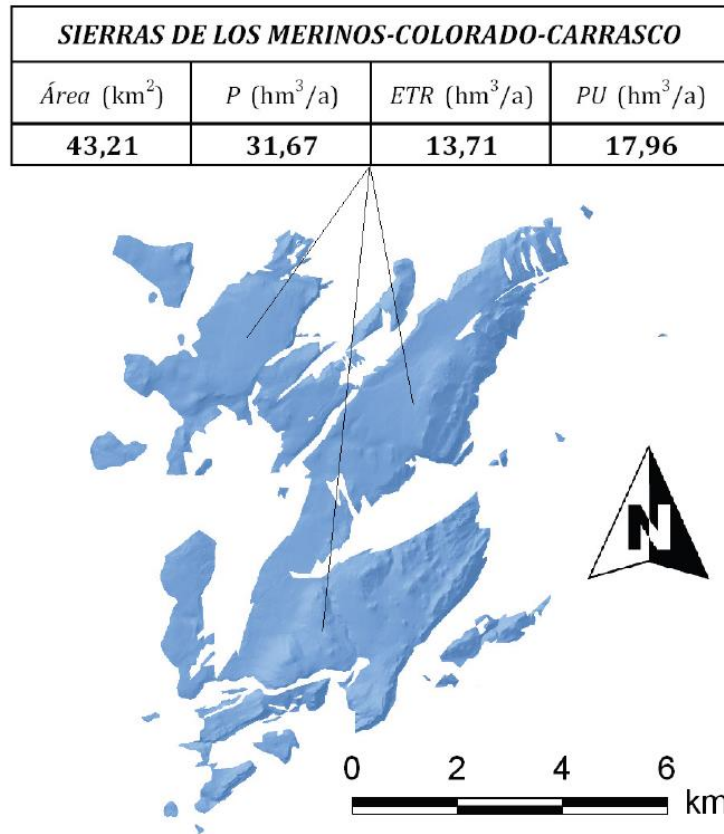


Figure 4.8 Mean values for water budget components at Merinos-Colorado-Carrasco test site for the historical period 1964/65-2009/10. Acronyms: P, precipitation; ETR, real evapotranspiration and PU, effective runoff (modified from Barberá, 2014).

On the other hand, in **Sierra de Ubrique** test site a mean annual precipitation in this area has been estimated around 1350 mm, however, it can variate depending on the altitude and sector from 900 mm to 1800 mm in the highest zones (Sánchez et al. 2015). Climatological and spring flow data from hydrological years 2012/13 (1997 mm annual precipitation), 2013/14 (1424 mm) and 2014/2015 (1020 mm), have been used to estimate mean effective rain (PU) (Fig. 4.9) for calculating water budget on this site (Martín-Rodríguez et al., 2016). This process has been realized through the use of Geographic Information System (GIS) tools by isohyet planimetry. Output flow has been measured in continuous by Odyssey® capacitance water level dataloggers. In a different way from the Merinos-Colorado-Carrasco site. Hargreaves method (Hargreaves and Samani, 1985) was used for ETP and Thornthwaite (1948) method was applied in this case for ETR estimation with soil water capacity equals to 50 mm. All these calculations realized with TRASERO v.2.1.0 resulted in an ETR mean annual value of 10,1 hm³.

No storage variations are assumed in historical analyses of water budget, so that the following equation has been applied for water budget calculations:

$$PU = (P - ETR)$$

As a result of applying this method, a mean annual effective runoff of 31,4 hm³ (Tab. 4.3) was estimated, and thus a recharge rate of 75% was obtained. However, despite this quite high value there is still a difference of 3,7 hm³ when compared with output values (35,1 hm³). This gap can be due to the fact that allogenic recharge was not taken into account for water balance or a possible connection to the Sierra del Endrinal aquifer system. Mean annual values obtained for this test site are summarized in Figure 4.10.

Preliminary Water Budget

Table 4.3 Mean recharge values calculated through water budget in soil (Hargreaves equation) with field capacity 50 mm for the 2012/13-2014/15 period (modified from Martín-Rodríguez et al., 2016).

| Acuífero | Superficie permeable (Km ²) | Precipitación total (PP), lluvia útil (PU) y evapotranspiración real (ETR). (hm ³) | | | | | | | | | Salidas (hm ³) | | | Media anual | Diferencia | | | |
|----------|---|--|------|------|---------|------|-----|---------|------|-----|----------------------------|---------|---------|-------------|------------|------|------|------|
| | | 2012/13 | | | 2013/14 | | | 2014/15 | | | Año hidrológico | | | | | | | |
| | | P | PU | ETR | P | PU | ETR | P | PU | ETR | 2012/13 | 2013/14 | 2014/15 | | | | | |
| Ubrique | 25,9 | 56,3 | 45,1 | 11,2 | 39,1 | 29,2 | 9,9 | 29,1 | 19,8 | 9,3 | 41,5 | 31,4 | 10,1 | 52,6 | 36,4 | 16,2 | 35,1 | -3,7 |

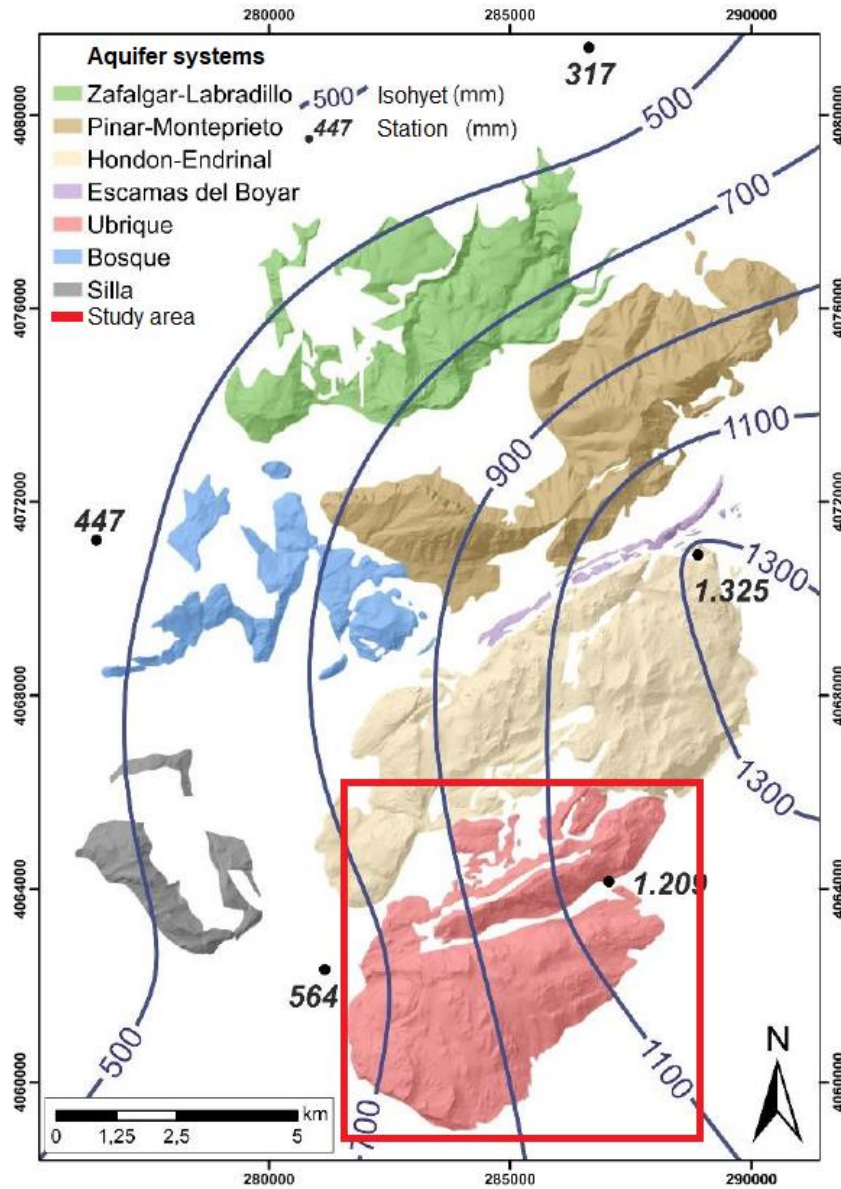


Figure 4.9 Mean hydrologic year spatial distribution of effective rain (PU) for pervious outcrops in 2012/13-2014/2015 study period (Modified from Martín-Rodríguez et al., 2016).

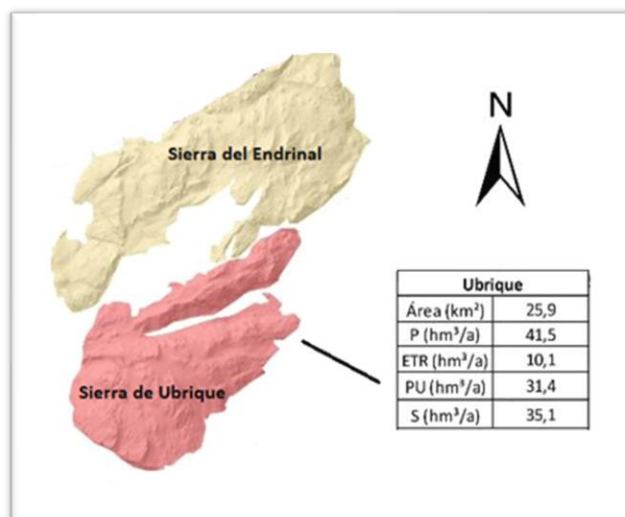


Figure 4.10 Mean values for water budget components at Sierra de Ubrique test site for the historical period 2012/13-2014/15. Acronyms: P, precipitation; ETR, real evapotranspiration; PU, effective runoff and S, output (modified from Martín-Rodríguez et al., 2016).

4.3 Discussion and Conclusion

Carbonate aquifers selected for test sites in Eastern Ronda Mountains are characterized by a small-scale recharge area, a high degree of karstification development and common geological features. **Merinos-Colorado-Carrasco** and **Sierra de Ubrique** aquifer systems have been studied in detail by researches carried out over the last 10 years approximately. Recharge area is well defined for both sites and water budget has previously been calculated as well with no big differences between input and output components. Main results are summarized in Table 4.4 and it suppose a reliable starting point to improve and update knowledge about hydrogeological features of the study area.

Table 4.4 Summary of main water budget results for different study periods at KARMA project study area.

| | Merinos-Colorado-Carrasco (Barberá, 2014) | Sierra de Ubrique (Martín-Rodríguez et al., 2016) |
|---|--|---|
| <i>Average rainfall</i> | 31,7 hm ³ /year | 41,5 hm ³ /year |
| <i>Recharge area</i> | 43,2 km ² | 25,9 km ² |
| <i>Net infiltration</i> | 18 hm ³ /year | 31,4 hm ³ /year |
| <i>Recharge rate (% Aver. Rainfall)</i> | 0,56 | 0,75 |
| <i>Average temperature</i> | 15,3 °C | 15,7 °C |
| <i>ETR</i> | 13,71 hm ³ /year | 10,1 hm ³ /year |
| <i>Output</i> | 17,0-24,3 hm ³ /year (various authors) | 35,1 hm ³ /year |

Further spatial distribution of recharge analysis could be realized in **Sierra de Ubrique** zone through the application of APLIS to standardize methods for estimating recharge rate, this will also permit to accurately estimate the allogenic recharge entering the aquifer at Villaluenga del Rosario shaft. In order to complete and improve underground flow knowledge in the study area selected for KARMA project, complementary monitoring activities such as continuous record of chemical parameters, spring discharge and water sampling will be carried out.

4.4 References

- Andreo, B., Vías, J., López-Geta, J.A., Carrasco, F., Durán, J.J. and Jiménez, P. (2004). *Propuesta metodológica para la estimación de la recarga en acuíferos carbonáticos*. Boletín Geológico y Minero 115 (2), 177-186.
- Andreo, B., Vías, J.M., Durán, J.J., Jiménez, P., López-Geta, J.A. and Carrasco, F. (2008). *Methodology for groundwater recharge assessment in carbonate aquifers: application to pilot sites in southern Spain*. Hydrogeology Journal 16 (5), 911-925.
- Barberá, J.A. and Andreo, B. (2012). *Functioning of a karst aquifer from S Spain under highly variable climate conditions, deduced from hydrochemical records*. Environ Earth Sci 65, 2337–2349.
- Barberá, J.A. (2014). *Investigaciones hidrogeológicas en los acuíferos carbonáticos de la Serranía Oriental de Ronda (Málaga)*. PhD Thesis. University of Málaga, Spain. 591 p.
- Barberá, J.A., Andreo, B. and Almeida, C. (2014). *Using non conservative tracers to characterize karstification processes in the Merinos-Colorado-Carrasco aquifer system (southern Spain)*. Environmental Earth Sciences 71 (2), 585-599.
- Cruz Sanjulián, J.J. (1974). *Estudio geológico del sector Cañete la Real-Teba-Osuna (Cordillera Bética, región occidental)*. PhD Thesis. University of Granada, Spain. 374 p.
- Goldscheider, N. and Drew, D. (2007). *Methods in Karst Hydrogeology*. Taylor & Francis, London (United Kingdom). 264 p.
- Hargreaves, G.H. and Samani, Z.A., (1985). *Reference crop evapotranspiration from temperature*. Transaction of ASAE 1(2): 96-99.
- IGME-GHUMA (2003). *Estudios metodológicos para la estimación de la recarga en diferentes tipos de acuíferos carbonáticos: aplicación a la Cordillera Bética*. Instituto Geológico y Minero de España, Madrid. 3 sections.
- Kessler, H. (1967). *Water balance investigations in the karstic regions of Hungary*. Symposium on Hydrology of Fractured Rocks, Dubrovnik (Yugoslavia), AIHS-UNESCO 1, 91-95.
- Marín, A.I. (2009). *Los Sistemas de Información Geográfica aplicados a la evaluación de recursos hídricos y a la vulnerabilidad a la contaminación de acuíferos carbonatados. Caso de la Alta Cadena (provincia de Málaga)*. PhD Thesis. University of Málaga, Spain. 131 p.
- Martín-Algarra, A. (2008). *El Subbético en las provincias de Málaga y Cádiz*. En: Vera, J.A. y Molina, J.M. (coord.). Proyecto Andalucía. Tomo 26. Geología II, 69-82. Publicaciones Comunitarias, Grupo Hércules. 376 p.
- Martín-Algarra, M. (1987). *Evolución geológica alpina del contacto entre las Zonas Internas y Externas de la Cordillera Bética*. PhD Thesis, University of Granada, Spain. 1171 p.
- Martín-Rodríguez, J.F., Sánchez-García, D., Mudarra-Martínez, M., Andreo-Navarro, B., López-Rodríguez, M., and Navas-Gutiérrez, M.R. (2016). *Evaluación de recursos hídricos y balance hidrogeológico en acuíferos*

kársticos de montaña. Caso de la Sierra de Grazalema (Cádiz, España). Book chapter on *Las aguas subterráneas y la planificación hidrológica*, 163-170. Spanish-Portuguese Congress. IAH Spanish Chapter. Madrid (Spain), November 2016.

Padilla, A. and Delgado, J. (2013). *Tratamiento y gestión de series temporales hidrológicas. Programa TRASERO 2.0*. Departamento de ciclo hídrico, Diputación Provincial de Alicante, 87 p.

Sánchez, D., Barberá, J.A., Mudarra, M. and Andreo, B. (2015). *Hydrogeochemical tools applied to the study of carbonate aquifers: examples from some karst systems of southern Spain*. *Environmental Earth Sciences*, 74, 199–215.

Thornthwaite, C. W. (1948). *An approach toward rational classification of climate*. *Geographical Review* 38 (1), 55-94.

Preliminary Water Budget

A perched aquifer is located within the upper Valanginian layer (marls and marly-limestones), superposing the Lez aquifer, though, both aquifers are regarded as mostly hydrogeologically unconnected. The Lez aquifer is connected vertically with a deep reservoir by deep faults (Bicalho et al., 2012). The groundwater that outflow from some springs that drain the Valanginian aquifer, notably Lauret, Dolgue and Lavabre springs infiltrate into the Lez karst system through localized infiltration zones along the Corconne-Les Matelles fault. Exchanges between the Lez karst system and surface water are poorly known as discharges through sinkholes have not been monitored. The boundaries of the Lez catchment vary with water level in the system. Besides, the response to extreme rainfall events depends on both soil moisture and water level.

As a large part of the hydrogeological catchment is relatively impermeable, due to the presence of marls and marly-limestones of the Valanginian, the Lez spring recharge area covers only 150 km². The main recharge area over the catchment corresponds to the Jurassic limestone outcrops located by the western and northern limits of the basin (Figure 3). Localized infiltration occurs through fractures and sinkholes along the basin and through the major geologic fault of Corconne-Les Matelles (located in the proximity of Claret well), in the northern part of the basin. A certain number of fractures are also known to exist only just upstream from the Lez spring.

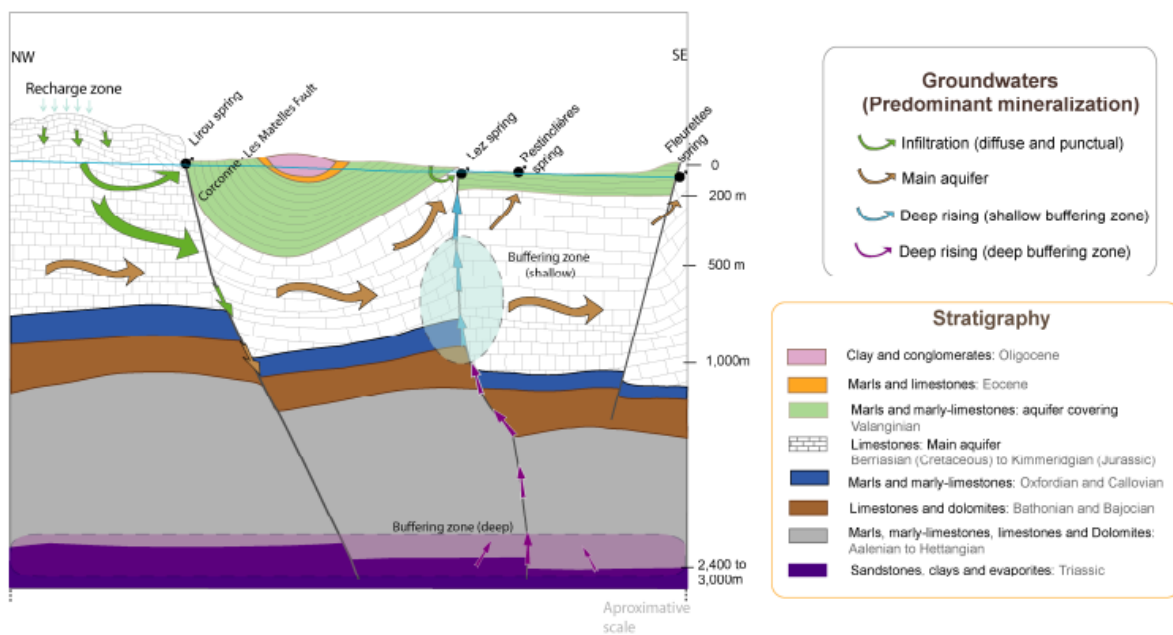


Figure 5.2 Simplified geological cross-section and conceptual model for groundwater circulation of the Lez karst system (after Bicalho et al., 2012).

The main outlet of the Lez karst system is the Lez spring. It used to be a perennial spring; however, since 1982 water has been directly withdrawn from the main conduit to supply Montpellier and its metropolitan region. The scheme of the pumping plant installation is shown in Figure 3. The pumping rate sometimes exceeds the natural water discharge in order to secure water supply throughout the year. Consequently, during low-water period, the spring dries out. Ecological water discharge at the Lez river is ensured during this period by a partial deviation of the pumped water to the river. The Lez karst system discharges also at several seasonal outlets: Lirou, Restinclières, Fleurette and Gour Noir (Figure 1). Lirou is a temporary spring that flows only 4 months in a year. Fleurette is the most ephemeral spring, flowing only a few weeks a year. Restinclières spring was perennial before the

Preliminary Water Budget

pumping, and according to recent field observations, it seems it remains a perennial spring despite the water exploitation.

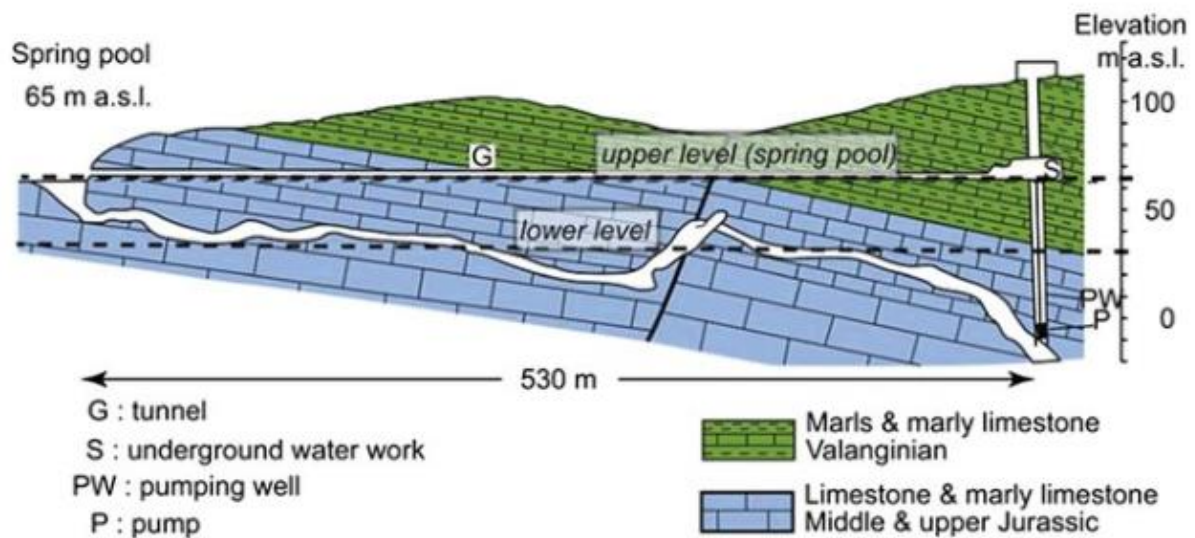


Figure 5.3 Cross section of the Lez spring, with the main conduit, the pumping station and the upper and lower groundwater levels (after Bakalowicz 2006).

5.2 Available Dataset

The following datasets are available in the Lez karst catchment to perform water budget estimation.

| Variable | Station | Period of availability | Data time step |
|-------------------------|---|------------------------|----------------|
| Rainfall | Meteo France | 8 * 8 km; all time | daily |
| Rainfall | 6 Meteorological stations around Montpellier | 1987 - 2019 | daily |
| Evapotranspiration | Mauguio (10 km south of Montpellier) | 1987 - 2019 | daily |
| Discharge | Lez spring | 2008 – 2019 | hourly |
| Pumping rate | Lez spring | 2008 - 2019 | hourly |
| Water table level | 8 boreholes scattered in the Lez karst system; 22 boreholes at a field site | since 1987 | hourly |
| Temperature | Lez spring | 2008 - 2019 | hourly |
| Electrical conductivity | Lez spring | 2008 - 2019 | hourly |

5.3 Preliminary water budget

The water budget of the Lez karst catchment consists of four major components: recharge, evapotranspiration, spring discharge and pumping at the Lez spring. The estimation of each component has been conducted by the French Geological Survey (BRGM; Caballero et al., 2015) with in-house codes Tempo and ESPERE. The estimation results have also been compared to that obtained by classical balance methods, such as Thornthwaite, Dingman-Penman and Dingman-Hamon. The estimated values for each component are reported below in detail.

Recharge

The Lez catchment is exposed to a Mediterranean climate, which is characterized by hot, dry summers, mild winters and wet autumns. Analyses by the Meteo France show that on average 40% of the annual precipitation occurs between September and November with a high variability across years. The estimated rainfall using Tempo fluctuates roughly between 50 mm and 850 mm depending on annual rainfall intensity. A high spatial variability also presents within the catchment (Mazzilli, 2011), ranging from 700 mm in the southeastern part of the catchment (Mauguio; Figure 1) to 1120 mm in the northwest (St-Martin-de-Londres). The average annual rainfall rate for the 1997/2005 period is 1037 mm based on a weighted average of the rainfall stations at Prades, Saint-Martin-de-Londres and Valflaunes (Figure 1; Fleury et al., 2009).

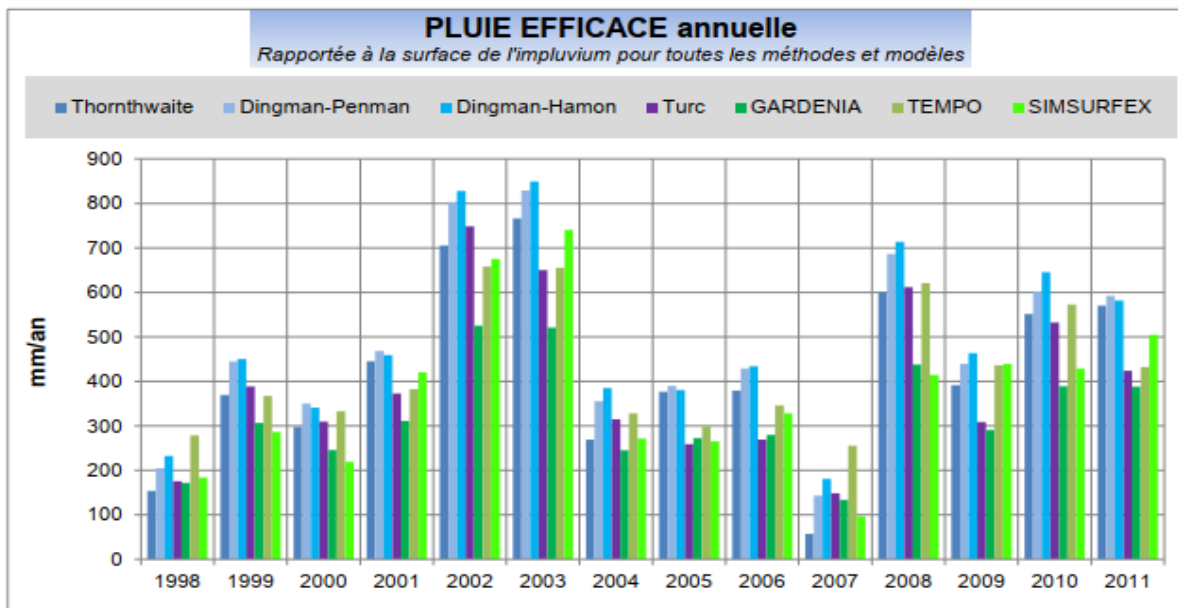


Figure 5.4 Estimated annual effective rainfall for the Lez karst system.

Since a large portion of the Lez karst system is covered by impermeable marls or marly limestone, the coefficient of effective rain infiltration is estimated to be between 60% and 65%. The annual recharge is estimated to be between 225 mm / year and 1169 mm / year, with an average interannual (over 20 years) of 585 mm / year.

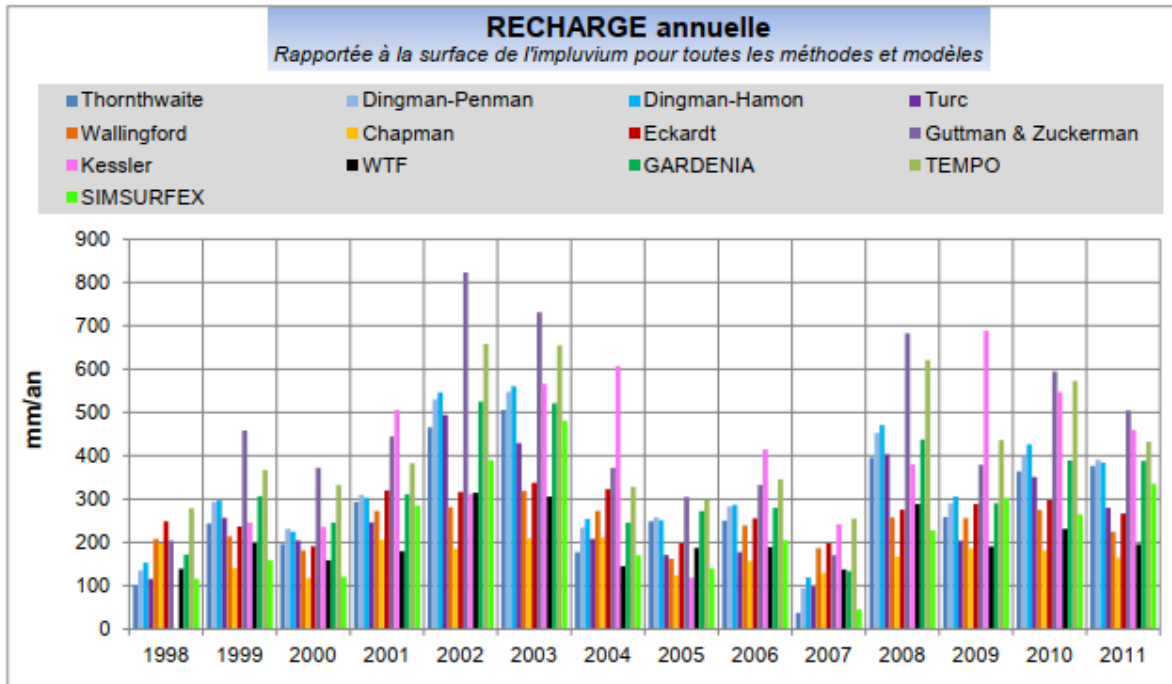


Figure 5.5. Estimation of recharge for the Lez karst system for the years between 1998 and 2011.

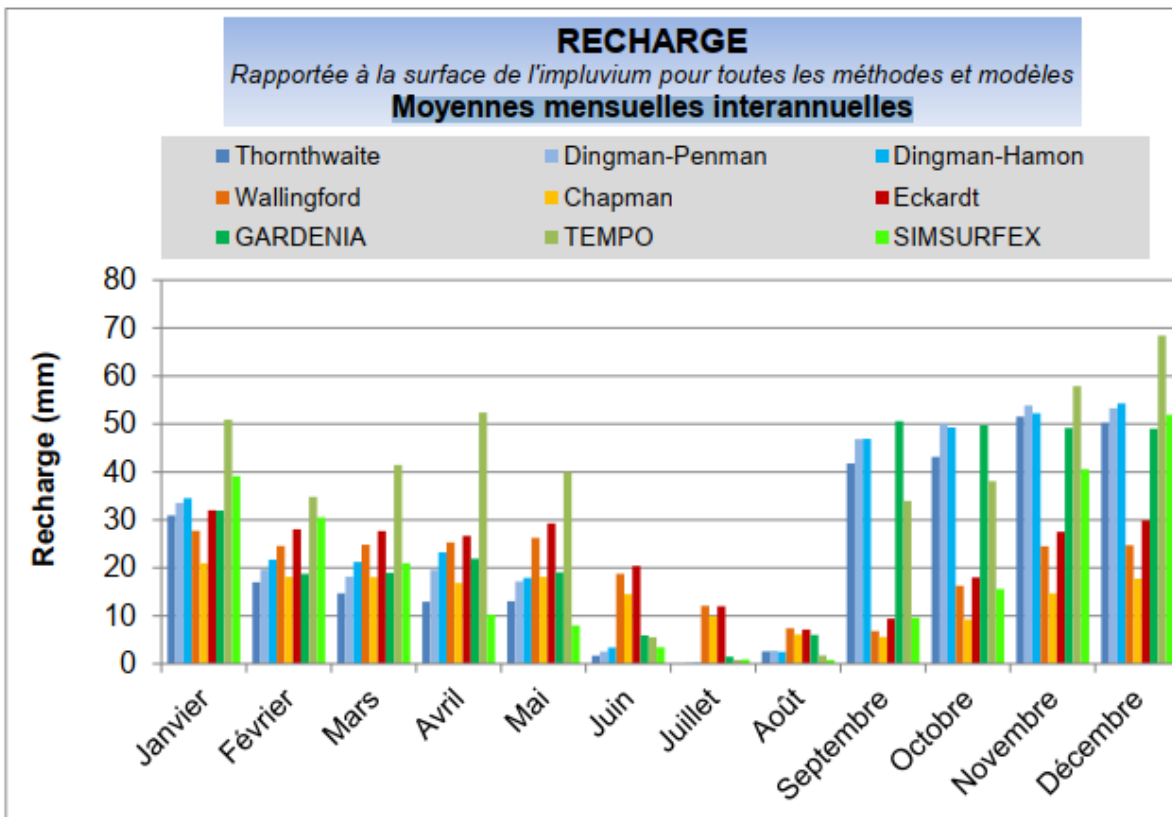


Figure 5.6 Estimated interannual monthly recharge for the years between 1998 and 2011.

Evapotranspiration

According to BRGM, the average annual evapotranspiration in the Lez karst catchment ranges from 388 mm to 572 mm. A daily potential evapotranspiration rate is estimated to be 1.1 mm/day using the Thornthwaite methods at the Montpellier Frejorgues meteorological station (Fleury et al., 2009).

Discharge

The Lez spring is the main perennial outlet of the system. The mean spring overflow discharge is an average $1.1 \text{ m}^3 \text{ s}^{-1}$ for the 1997-2005 period. The minimum spring discharge is 160 l/s (return flow). The maximum spring discharge is $16 \text{ m}^3 \text{ s}^{-1}$ (1997-2005 period). The discharge measurement uncertainty is estimated to be about $\pm 5\%$. The pumping rate is in average $1.1 \text{ m}^3 \text{ s}^{-1}$ over the 1997-2005 period. The pumping rate measurement uncertainty is estimated to be negligible. The minimal piezometric level within the karst conduit is 38 m ASL for the 1997-2005 period, with an average 147 days of overflow per year. The water level measurement uncertainty is estimated to be negligible (Mazzilli et al, 2011).

Pumping

The Lez aquifer is subject to "active management" (Avias, 1995; Figure 3), which means that the flows pumped in low water (1,200 to 1,700 l/s) are higher than those pumped in high water (900 l/s). This type of management, which makes it possible to maximize the exploitation of the aquifer, is made possible thanks to the high recharge capacity of the aquifer, especially thanks to fall precipitation. The maximum pumping rate is fixed at 1700 l/s, with a level minimum water set by prefectural authorization at 35 m NGF (the overflow threshold of the source is located 65 m NGF). A reserved flow of 160 l/s is returned to the Lez river downstream of the source, when it does not overflow.

5.4 References

- Avias, J. (1995). Gestion active de l'exurgence karstique de la source du Lez. Dans: Hydrogéologie 1, p. 113-127. Cf. p. v, ix, xvii, 90, 93, 134.
- Bakalowicz, M. (2006), Causses Majeurs. In: Roux, J.C. (ed.) Aquifères et eaux souterraines en France. BRGM Éditions & CFH-AIH, Orléans
- Bicalho, C. C., Batiot-Guilhe, C., Seidel, J. L., Van Exter, S., & Jourde, H. (2012), Geochemical evidence of water source characterization and hydrodynamic responses in a karst aquifer. *Journal of Hydrology*, 450, 206-218.
- Caballero, S., Lanini, S., Seguin, J. J., Charlier, J. B. and Olivier, C. (2015), Caractérisation de la recharge des aquifères et évolution future en contexte de changement climatique – application du bassin Rhone Méditerranée Corse, BRGM/RP-64779-FR.
- Marechal, J. -C., Vestier, A., Jourde, H. and Dorfliger, N. (2013), L'hydrosystème du Lez : une gestion active pour un karst à enjeux. *Karstologia*, No. 62, 1-6.
- Mazzilli N. (2011). Sensibilité et incertitude de modélisation sur les bassins versants à forte composante karstique, PhD thesis, Université Montpellier II, Sciences et Techniques du Languedoc, 210p.
- Mazzilli, N., Guinot, V., & Jourde, H. (2010), Sensitivity analysis of two-dimensional steady-state aquifer flow equations. Implications for groundwater flow model calibration and validation. *Advances in water resources*, 33(8), 905-922.

- P. Fleury, B. Ladouche, Y. Conroux, H. Jourde, N. Dörfliger (2009). Modelling the hydrologic functions of a karst aquifer under active water management – The Lez spring. *Journal of Hydrology*, Elsevier, 2009, 365 (3-4), p. 235-243. 10.1016/j.jhydrol.2008.11.037.
- Thiery, D., and Berard, P. (1983), Alimentation en eau de la ville de Montpellier - captage de la source du Lez - études des relations entre la source et son réservoir aquifère. Rapport BRGM n° 83 SGN 167 LRO.

6. Djebel Zaghouna aquifer, Tunisia

6.1 Field site description

The Zaghouna massif extends from the East-west extension valley of the Rmal wadi in the north, to the transversal syncline of Loukanda which follows, in the south, the bridge road from Fahs to Saouaf-Infidha city (fig.1). It is made up of a series of Jurassic points, the most important of which is in the north, the Djebel Zaghouna, our field of study.

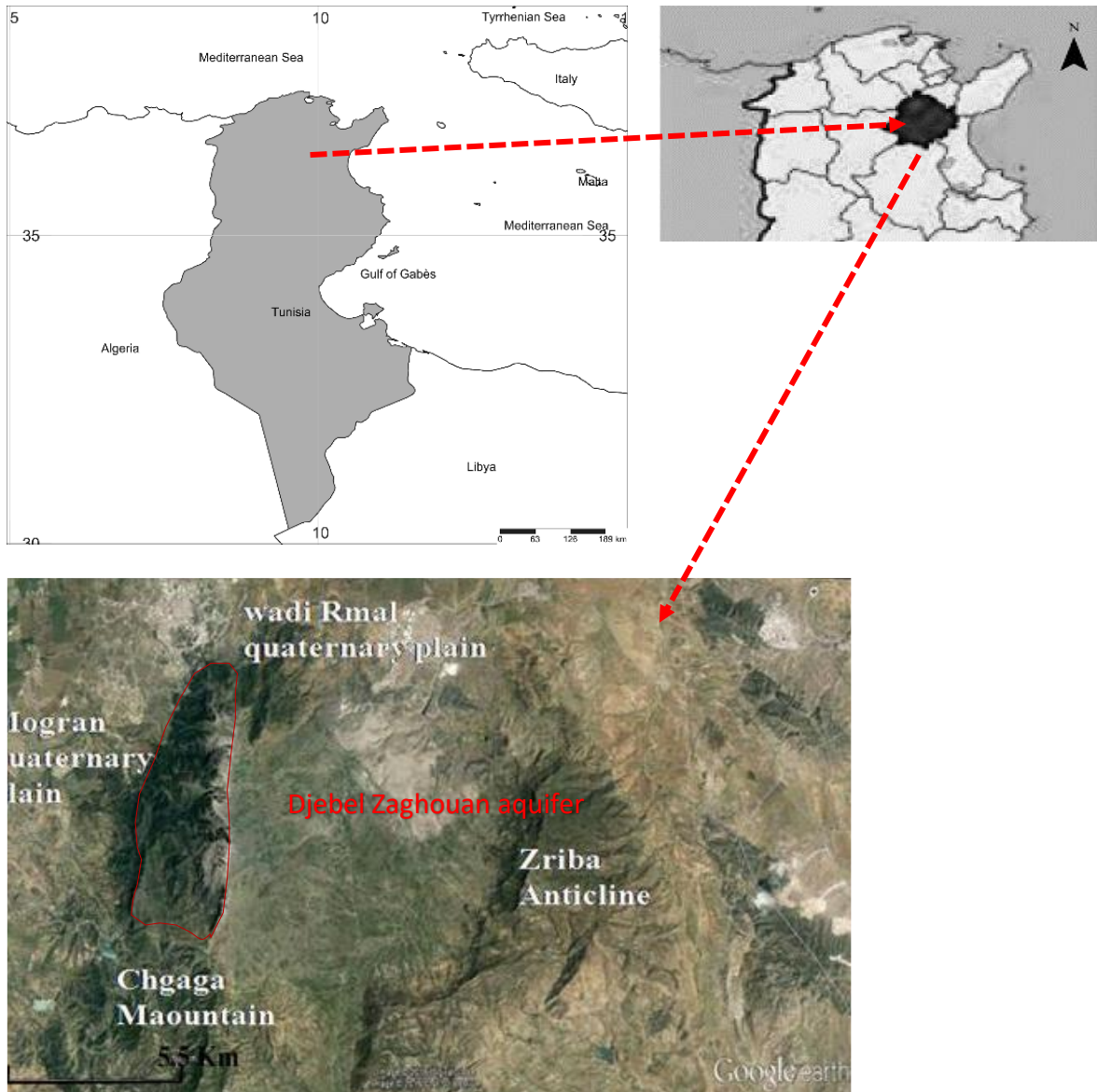


Fig. 6.1: Location of the Djebel Zaghouna aquifer.

The region of Zaghouna is characterized by an upper semi-arid to subhumid climate with an average annual rainfall of 467 mm presenting heterogeneous spatial distribution and a large time fluctuation (from 245 to 625 mm). The average annual temperature is about 17.7°C.

The Zaghouna anticline is mainly constituted by Jurassic limestone. It's limited by the rock-fall and the cretaceous formations. The fig. 2 shows that the geology of the Djebel is characterized by the presence of southern and transverse faults that have created individualized blocks. These faults which allow an infiltration of meteoric waters are between jumps: the Kef El Orma fault, the Great Peak fault and the Achilles fault.

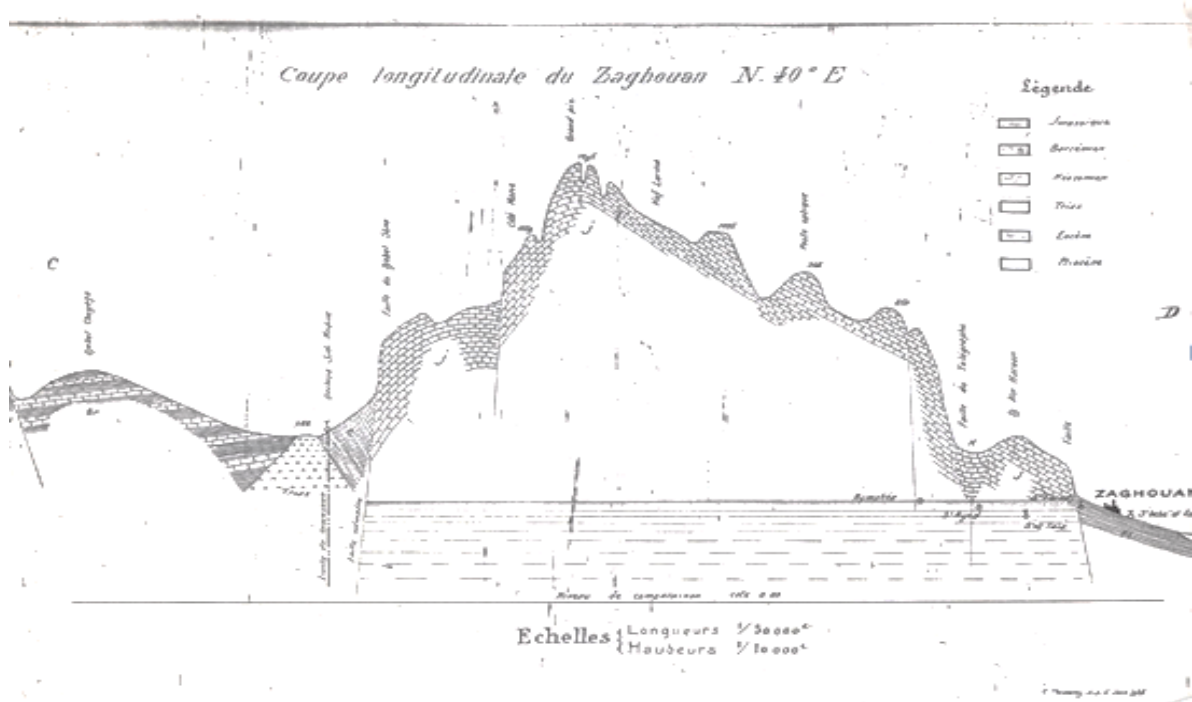


Fig. 6.2 Geological context of Djebel Zaghouan (Castany, 1951).

The Jurassic limestone block is a trapezoidal, cavernous and fissured limestone with a longitudinal dimension of about 8 km along a north to 40°East direction, and an average of 2.4 km in the transverse direction, along a north to 45°West direction. It has a surface area of 19 km² at the altitude of 300 m NGT. The massif is surrounded by marly soil acting as a watertight barrier and can be subdivided into 3 compartments running from north to south.

- Small Zaghouan which gives birth to Ain Haroun.
- Transmission station massifs, Kef El Orma, Kef El Blidah and Djebel Stâa; they are the most extensive compartment, which give rise to the most important springs including Water temple (Nymphaeum), Ain Ayed and Ain Oued El Guelb.
- The great peak massif which gives birth to the source of Sidi Medina.

The general dip of the limestone layers and the topographical configuration towards the north-west explain the presence and importance of the springs of both slope and east massif.

The massif contains 14 springs. The most important springs are on massif north-western slope among them: Nymphaea, Ain Ayed, Ain ElGuelb, Gallerie 44 and Gallerie 47 and Ain Haroun, shown in fig.3.

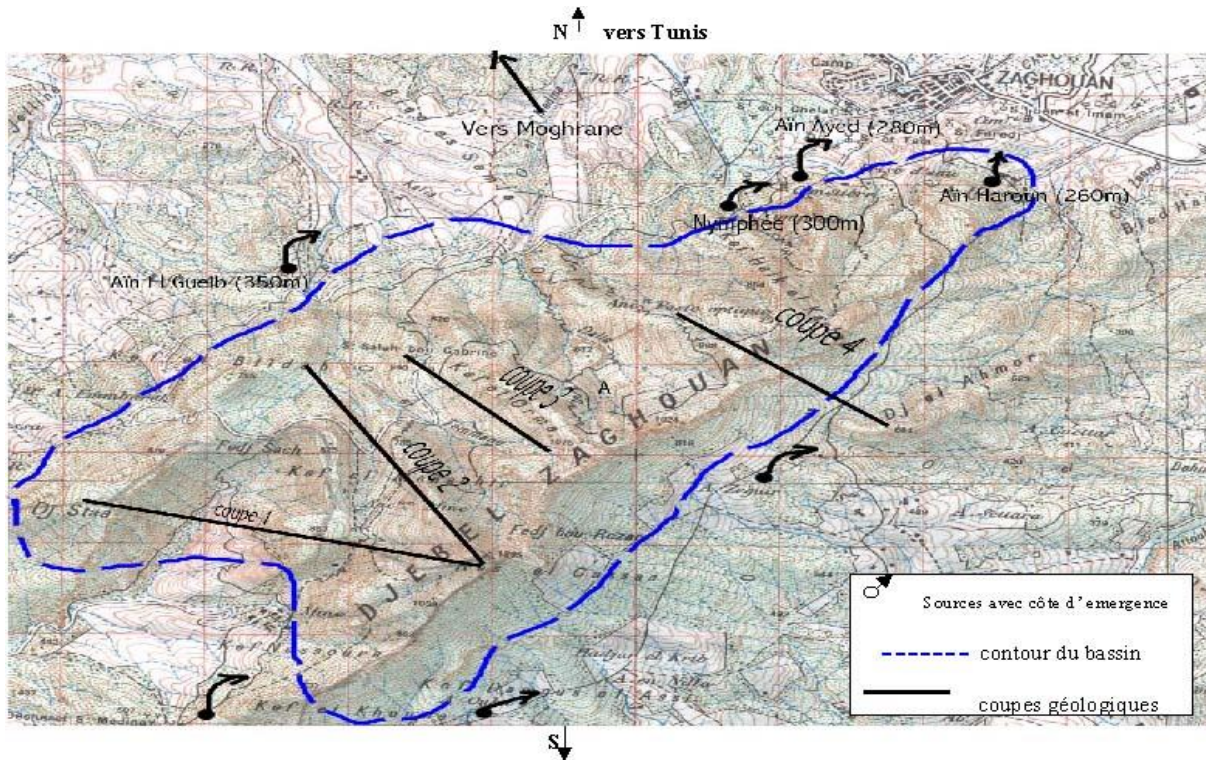


Fig.3. Springs location map (extract Zaghouan map n°25 at scale 1:50000).

6.2 Water resources

Djebel Zaghouan limestone aquifer is the one of the most important water resources of good quality in the region. Since the roman era, the karst springs of Zaghoau, supplied drinking water for the local cities and for the capital (Carthage then Tunis) through an aqueduct of 132 km. Due to the drought of the forties, three galleries (known as 44 and 47) were drilled in the system (fig.4) to drain the natural resurgences. These two galleries are about 300 m long. They are all equipped with control valves that allow consumers to be served according to their needs. A series of boreholes were also installed from the nineties.



Gallery 44



Gallery 47

Fig.6.4. Photos of Galleries 44 and 47 (field trip February 2019 and Dziri, 2016).

Preliminary Water Budget

Currently, the aquifer is exploited by mainly 9 boreholes and galleries intended for the drinking water supply of the city of Zaghouan and the surrounding rural agglomerations. Three of these wells used as commercialized mineral water (Cristaline, Aqualine and Prestine).

Since galleries 44 and 47 are dry and to cope with water shortage that Zaghouan city suffers from, two other boreholes (Water temple and Ain Haroun 3bis) were drilled in 2017 and 2018.

6.3 Preliminary water budget

The preliminary water budget will be principally based on the modelling study performed by Djebbi et al. (2001) and Sagna (2000). This study proposed to assess the water balance and to quantify the storage capacity of the aquifer associated with the Jurassic limestones of Djebel Zaghouan,

The available flow data corresponding to the natural flow period was recorded from 1915 to 1927. Table 1 and 2 presents the Zaghouan springs production before the digging of the galleries and Zaghouan springs production with exploitation by the galleries respectively. The natural flow period was marked by heavy rainfall of the 1920-1921 and a low rainfall during the 1926-1927 hydrological years, which resulted into high spring flow (6.5 Mm³) a very low flow of 1.9 Mm³ respectively. These observations are in conformity with the natural flow of the resurgences during this period.

Table 6.1 Zaghouan springs production before exploitation by the galleries.

| Production (Mm ³) | |
|-------------------------------|------------|
| Year | Total |
| 1915-1916 | 3.5 |
| 1916-1917 | 3.3 |
| 1917-1918 | 3.3 |
| 1918-1919 | 3.7 |
| 1919-1920 | 3 |
| 1920-1921 | 6.5 |
| 1921-1922 | 4.8 |
| 1922-1923 | 3.9 |
| 1923-1924 | 3.8 |
| 1924-1925 | 2.9 |
| 1925-1926 | 3 |
| 1926-1927 | 1.9 |
| Average | 3.6 |
| Standard deviation | 1.1 |

Table 6.2 Zaghouan springs production with exploitation by the galleries.

| Production (Mm ³) | |
|-------------------------------|------------|
| Year | Total |
| 1970-1971 | 4 |
| 1971-1972 | 3.9 |
| 1972-1973 | 5 |
| 1973-1974 | 5.9 |
| 1974-1975 | 4.2 |
| 1975-1976 | 3.7 |

| Production (Mm ³) | |
|-------------------------------|------------|
| Year | Total |
| 1976-1977 | 3.2 |
| 1977-1978 | 2.4 |
| 1978-1979 | 1.9 |
| 1979-1980 | 1.3 |
| 1980-1981 | 1.5 |
| 1981-1982 | 2.4 |
| 1982-1983 | 6.2 |
| 1983-1984 | 2.9 |
| 1984-1985 | 3.3 |
| 1985-1986 | 2.9 |
| 1986-1987 | 2.1 |
| 1987-1988 | 1.9 |
| 1988-1989 | 1.6 |
| 1989-1990 | 1.9 |
| 1990-1991 | 3.3 |
| 1991-1992 | 4.2 |
| 1992-1993 | 3.4 |
| 1993-1994 | 2.9 |
| 1994-1995 | 1.9 |
| | |
| Average | 3.1 |
| Standard deviation | 1.3 |

Sagna (2000) considered the most continuous and overlapping series of both dry and wet years. The average interannual rainfall calculated over a time series of 47 years (table 5) was 501 mm with a standard deviation of 170 mm. Observations were recorded at the TPSM rainfall station. Temperature was taken from bibliography and monthly mean evapotranspiration were calculated using Thornwaith formula.

Djebbi et al. (2001) and Sagna (2000) also developed a conceptual deterministic model to transform the rainfall received by the calcareous solid mass into the sum of the discharge flows (springs and galleries). The model was validated using meteorological and hydrodynamic collected data. Calculation time step is daily, and the structure of the model is the following (fig.5):

- Two inputs: rainfall and evapotranspiration.
- A production function and transfer function which transform the precipitation received by the massif into flows at the discharge and which modulate the distribution of these flows over time.
- One output: the total calculated discharge flow. The processes taking place in each reservoir zone are described by a specific water balance equation. These equations make it possible to determine, at the end of each time step, the level of filling of each reservoir zone, the exchanges by infiltration or percolation between zones, and the losses of the system (real evapotranspiration and surface runoff).

Preliminary Water Budget

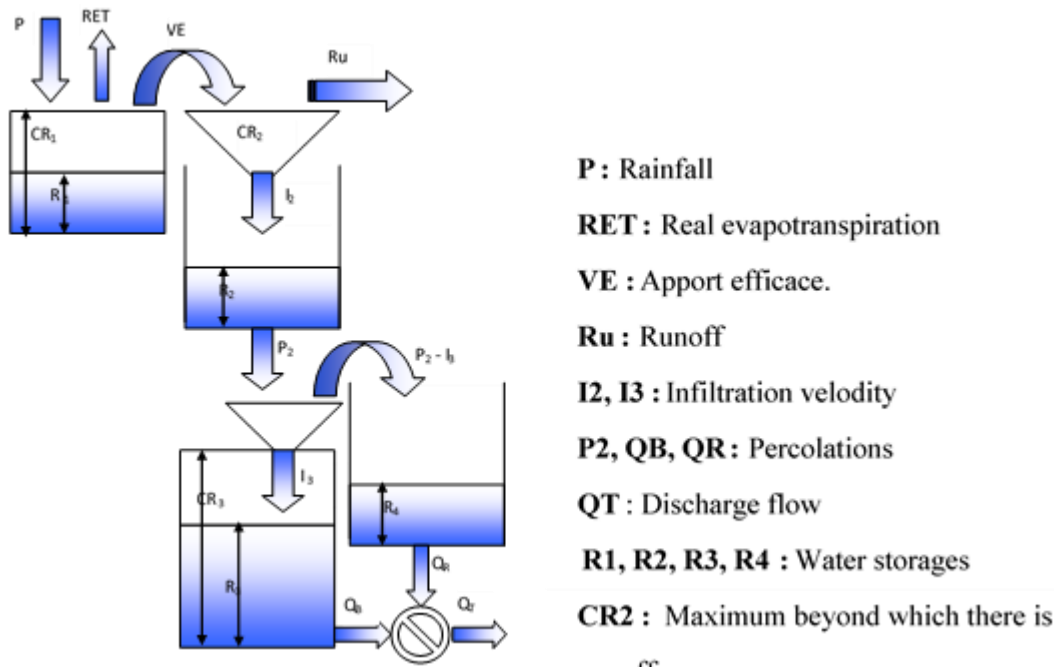


Fig.6.5 The conceptual Model.

Model was run for a calibration period corresponding to the natural functioning of the system from 1915 to 1927 and a validation period from 1970 to 1995 including the aquifer exploitation via galleries and wells. The performance of the model was acceptable with a Nash criterion ranging between 0.54 % and 0.77 %.

Tables 3 and 4 provides Djebel Zaghouan water budgets summary (rainfall, infiltration rate, runoff and evapotranspiration) for the calibration and the validation period respectively. It provides (all of which represent the components of a natural water budget (1915-1927)) (SAGNA,2000), after the classical methodology of calibration and final validation in the model.

Table 6.3 Water budget for the calibration period (1915-1927).

| Year | rainfall (mm) | flow (Mm3/an) | RET (Mm3) | Runoff (Mm3) | water budget (%) | infiltration coef (%) |
|----------------|---------------|---------------|-----------|--------------|------------------|-----------------------|
| 1915-1916 | 480 | 3.4 | 4.5 | 0.37 | 110 | 38 |
| 1915-1917 | 461 | 3 | 6.1 | 0.21 | 93 | 35 |
| 1915-1918 | 442 | 3 | 4.8 | 0.29 | 103 | 36 |
| 1915-1919 | 550 | 4 | 4.8 | 0.45 | 113 | 38 |
| 1915-1920 | 347 | 3 | 4.7 | 0.15 | 83 | 47 |
| 1915-1921 | 867 | 5.2 | 7.1 | 0.75 | 126 | 31 |
| 1915-1922 | 393 | 5 | 3.4 | 0.32 | 84 | 68 |
| 1915-1923 | 400 | 4 | 4.1 | 0.28 | 91 | 53 |
| 1915-1924 | 525 | 4.4 | 4.8 | 0.41 | 103 | 45 |
| 1915-1925 | 380 | 3.4 | 4.8 | 0.2 | 86 | 48 |
| 1915-1926 | 520 | 2.9 | 7 | 0.21 | 95 | 30 |
| Average | 488 | 3.8 | 5.1 | 0.33 | 99 | 43 |

Table 6.4 Water budget validation of model (1970-1995).

| Year | rainfall (mm) | flow (Mm ³ /an) | RET (Mm ³) | Runoff (Mm ³) | water budget (%) | infiltration coef (%) |
|-----------|---------------|----------------------------|------------------------|---------------------------|------------------|-----------------------|
| 1970-1971 | 448 | 4.3 | 3.2 | 0.42 | 93 | 50 |
| 1971-1972 | 642 | 5.3 | 5.7 | 0.51 | 94 | 43 |
| 1972-1973 | 686 | 6 | 5.2 | 0.6 | 92 | 46 |
| 1973-1974 | 547 | 5.9 | 4.9 | 0.4 | 108 | 57 |
| 1974-1975 | 472 | 4.7 | 4.6 | 0.3 | 109 | 53 |
| 1975-1976 | 506 | 4 | 6.2 | 0.3 | 110 | 42 |
| 1976-1977 | 341 | 3 | 4.1 | 0.2 | 114 | 48 |
| 1977-1978 | 373 | 2.5 | 5.1 | 0.16 | 110 | 35 |
| 1978-1979 | 352 | 2.3 | 4 | 0.2 | 98 | 34 |
| 1979-1980 | 425 | 1.9 | 6.7 | 0.1 | 108 | 23 |
| 1980-1981 | 339 | 1.9 | 4.3 | 0.17 | 99 | 30 |
| 1981-1982 | 409 | 2.3 | 4.6 | 0.25 | 92 | 30 |
| 1982-1983 | 641 | 5.5 | 3.4 | 0.7 | 79 | 46 |
| 1983-1984 | 252 | 2.7 | 4.6 | 0.02 | 154 | 57 |
| 1984-1985 | 551 | 3.2 | 5.8 | 0.37 | 90 | 31 |
| 1985-1986 | 334 | 2.5 | 4.5 | 0.15 | 113 | 40 |
| 1986-1987 | 498 | 3 | 5.7 | 0.3 | 96 | 33 |
| 1987-1988 | 232 | 1.6 | 4.4 | 0 | 137 | 37 |
| 1988-1989 | 273 | 1 | 4.1 | 0.05 | 101 | 21 |
| 1989-1990 | 609 | 2.5 | 7 | 0.39 | 86 | 21 |
| 1990-1991 | 567 | 4.4 | 4.3 | 0.52 | 85 | 40 |
| 1991-1992 | 687 | 4.8 | 7.6 | 0.44 | 98 | 37 |
| 1992-1993 | 463 | 3.8 | 5.6 | 0.26 | 110 | 44 |
| 1993-1994 | 292 | 2.7 | 4.1 | 0.1 | 126 | 49 |
| 1994-1995 | 192 | 1.4 | 3.6 | 0 | 138 | 38 |
| Average | 445 | 3.3 | 4.9 | 0.28 | 106 | 39 |

6.4 Conclusion

An overview of the Djebel Zaghoun aquifer geological, climatic and exploitation characteristics was described in the present report. The estimation of the water budget was based on a previous modelling study that was also detailed. The following steps are to collect and update the exploitation data and to set up the adequate experimental and modelling tasks in order to check and update the previous calculations of the water budget by also improving the knowledge of recharge areas and rates and evapotranspiration estimation.

6.5 References

- Castany, G. (1951). Geological study of the Tunisian eastern atlas, Besançon. Imp de l'IEST
- Djebbi, M., Sagna J. and Besbes M. (2001). Sources karstiques de Zaghoun : Recherche d'un opérateur Pluie – Débit. Sciences Et Techniques De L Environnement Memoire Hors Serie,
- Dziri, R., Chkir N., Emblanch C., Zouari K. and Gallali A. (2016). Geochemical and hydrodynamic characteristics of the karstic system of Jbal Zaghoun (Northeastern-Tunisia). I-DUST 2016: inter-Disciplinary Underground Science & Technology Avignon

- Nazoumou, Y. (2002). Study of the deep aquifers of the South-Eastern Governorate of Zaghouan (Tunisia). Report, Water Resources Directorate /SCET-Tunisia, Tunis, TUNISIA, 100 p.
- Nazoumou, Y. (2002). Water resources database of the South Delegations- East of the Governorate of Zaghouan (Tunisia). Report, Directorate of Resources in Water / SCET-Tunisia, Tunis, TUNISIA, 100 p.
- Sagna, J. (2000), Study and modeling of Zaghouan karst sources, Master thesis. ENIT. 84 p.